with $NaBH_4$ prior to *O*-glycan releasing reaction is necessary. An aqueous solution of 2 M $NaBH_4$ (500 μl) was added to the supernatant and kept at room temperature for 30 min. Glacial acetic acid was carefully added to the mixture to decompose excess $NaBH_4$, and the mixture was passed through an ultrafiltration membrane (5000 MWCO [molecular weight cutoff], Amicon Ultra, Millipore) at 10,000g. The mixture of glycopeptides on the membrane was dissolved in water (100 μl) and used for releasing reaction of *O*-glycans from mucin-type glycoproteins and proteoglycans.

Releasing reactions of O-glycans

Releasing reaction of *O*-glycans using the automated glycan releasing system was performed according to the method reported previously [9]. Briefly, an aqueous solution of 0.5 M LiOH was used as the releasing reagent and the eluent. To the flow of the eluent at 1.0 ml/min, an aqueous solution of the mixture of glycopeptides from each cell line (5.0×10^6 cells/50 μl) obtained as described above was injected. After the sample solution was mixed with the eluent in the mixing device, the mixed solution was moved to the reactor kept at 60 °C, in which a reaction tube (0.25 mm i.d., 10 m length, 700 μl volume) was set. During passing through the reaction tube in the reactor, *O*-glycans were released from the peptide. The eluate containing the reaction mixture from the reactor was immediately introduced to a cartridge (1.0 ml volume) packed with cation exchange resin and collected to a fraction collector installed in the system while monitoring the absorbance at 230 nm. The collected solution containing the released *O*-glycans was evaporated to dryness by a centrifugal evaporator, and the dried material was used for fluorescent labeling with 2AA.

Fluorescent labeling of the released O-glycans with 2AA

The mixture of the released *O*-glycans was dissolved in 2AA solution (200 μl), which was freshly prepared by dissolution of 2AA (30 mg) and sodium cyanoborohydride (30 mg) in methanol (1 ml) containing 4% sodium acetate and 2% boric acid. The mixture was kept at 80 °C for 1 h. After cooling, water (100 μl) was added and the mixture was applied to a column of Sephadex LH-20 (1.0 cm i.d., 30 cm length) previously equilibrated with 50% aqueous methanol. The earlier eluted fluorescent fractions were pooled and evaporated to dryness under reduced pressure. The dried residue was dissolved in water (40 μl), and a portion (20 μl) was injected to analyze by serotonin affinity chromatography.

Serotonin affinity chromatography for separation of O-glycans and GAGs

Mucin-type glycans and GAGs are analyzed according to the procedures (see Supplementary Fig. 2 in supplementary material). Serotonin affinity chromatography for group separation of glycans based on the number of attached sialic acid residues was performed with a Jasco HPLC apparatus equipped with two PU-980 pumps and a Jasco FP-920 fluorescence detector (Tokyo, Japan) using a serotonin-immobilized column (4.6 × 150 mm) with linear gradient from water (solvent A) to 50 mM ammonium acetate (solvent B) at a flow rate of 0.5 ml/min. Initially solvent B was used at 5% concentration for 2 min, and then linear gradient elution was performed to 37% B for 16 min. After collecting mucin-type glycans, an aqueous solution of 1 M NaCl was used to elute GAGs during the subsequent 15 min. The column was then equilibrated with the starting eluent. After group separation, mucin-type glycan fractions were analyzed by MALDI–TOF MS and normal phase HPLC (NP–HPLC). In addition, GAG fractions were digested with specific eliminases and analyzed by CE after labeling with 2AA.

HPLC analysis of mucin-type glycans

The apparatus was the same as described above. Separation was done with a TSK-GEL Amide-80 column (Tosoh, 4.6 × 250 mm) using a linear gradient formed by 0.1% acetic acid in acetonitrile (solvent A) and 0.2% acetic acid in water containing 0.1% triethylamine (solvent B) at 40 °C. The column was initially equilibrated and eluted with 85% solvent A for 2 min, from which point solvent B was increased to 50% over 80 min at 1.0 ml/min. Then, the column was washed with 90% B for 10 min and equilibrated at initial conditions for 15 min. The amounts of mucin-type glycans were calculated from the peak areas based on the standard curve prepared using maltopentaose labeled with 2AA.

MALDI–TOF MS analysis of mucin-type glycans separated by serotonin affinity chromatography

MALDI–TOF MS spectra of 2AA-labeled glycans were acquired on a Voyager-DE Pro mass spectrometer (PE Biosystems, Framingham, MA, USA) in negative or positive ion linear mode with a nitrogen laser (338 nm) for the ionization source. Accelerating voltage was set at 20 kV, and delayed extraction was performed after 800 ns. DHB was used as matrix material throughout the work. The mass numbers of the molecular ion peaks were corrected using a mixture of 2AA-labeled dextran oligomers as standard mass markers. The sample solution (1 μl) was mixed with 2% DHB (1 μl) in ethanol on a stainless-steel plate, and the mixture was dried under atmosphere at room temperature.

MS^n analysis of mucin-type glycans

Structures of mucin-type glycans were confirmed by the MS^n technique on a MALDI–quadrupole ion trap–TOF mass spectrometer (AXIMA-Resonance, Shimadzu, Kyoto, Japan). Acquisition and data processing were controlled by Launchpad software (Kratos Analytical, Manchester, UK). For collision-induced dissociation, argon was used as the collision gas. For the sample preparation, a 0.5-μl volume of the matrix solution (DHB, 10 mg/ml in 30% ethanol) was deposited on the stainless-steel target plate and allowed to dry. Then, a portion (0.5 μl) of the appropriately diluted analyte solution (typically ~1 pmol/μl) was applied to cover the matrix on the target plate and allowed to dry.

Analysis of GAGs collected by serotonin affinity chromatography

After collecting the GAG pool by serotonin affinity chromatography, the GAG pool was passed through a filter device (3000 MWCO). Half of the GAG mixture on the membrane was dissolved in 50 mM Tris–HCl buffer (pH 8.0, 100 μl). Chondroitinase ABC (0.5 U) dissolved in the same buffer (10 μl) was added to the solution and kept at 37 °C overnight. The other half of the GAG mixture was dissolved in 100 mM sodium acetate/0.1 mM calcium acetate (pH 7.0, 100 μl). Heparitinases 1 and 2 (5 mU/10 μl each) were added to the solution, and the mixture was kept at 37 °C overnight. Both reaction mixtures obtained by digestion with chondroitinase ABC and heparitinases were labeled with 2AA and analyzed by CE.

CE analysis of unsaturated disaccharides from GAGs

CE was performed on a P/ACE MDQ Glycoprotein System (Beckman Coulter, Fullerton, CA, USA) equipped with a helium–cadmium laser-induced fluorescence detector (excitation 325 nm, emission 405 nm). For the analysis of 2AA-labeled unsaturated disaccharides derived from GAGs, electrophoresis was performed with a fused silica capillary (50 μm i.d. × 30 cm) in 100 mM Tris–phosphate buffer (pH 3.0). Sample solutions were introduced into

the capillary by pressure injection at 1 psi for 10 s. Separation was performed by applying the potential of 25 kV at 25 °C.

The amounts of unsaturated disaccharides were calculated from the peak areas based on the standard curve prepared using standard samples of unsaturated disaccharides labeled with 2AA.

Results and discussion

Separation of mucin-type glycans and GAGs by serotonin affinity chromatography

We have been employing serotonin affinity chromatography for group separation of 2AA-labeled *N*- and mucin-type glycans prepared from various cancer cell lines using gradient elution with ammonium acetate. The separation is achieved based on the number of sialic acid residues [2,38], and the glycans separated in this way are analyzed by HPLC and MS without further purification steps because the glycan fractions are in an aqueous solution of volatile salts at low concentrations. This is one of the advantages of serotonin affinity chromatography.

During the studies on the analysis of the released glycans, we found that GAGs are also retarded on a serotonin-immobilized column (Fig. 1). An example for the analysis of oligomers derived from hyaluronan (HA oligomers) is shown in Fig. 1A. HA oligomers were strongly retained on the serotonin-immobilized stationary phase based on their total negative charges (i.e., oligomers having the higher molecular weight are eluted later). It is considered that glucuronic acid residues in HA molecules play important roles in interaction with serotonin. We also analyzed the artificial mixture of mucin-type glycans from fetuin and HA oligomers (Fig. 1B). Mucin-type glycans from fetuin were observed at 8 and 15 min, and then HA oligomers were observed. The results indicated that serotonin affinity chromatography is useful for group separation of mucin-type glycans and GAGs. Based on these results, we developed the procedures for one-pot analysis of mucin-type glycans and GAGs as described in Materials and methods and applied the method to the analysis of *O*-glycans on HCT116 cells (colorectal adenocarcinoma).

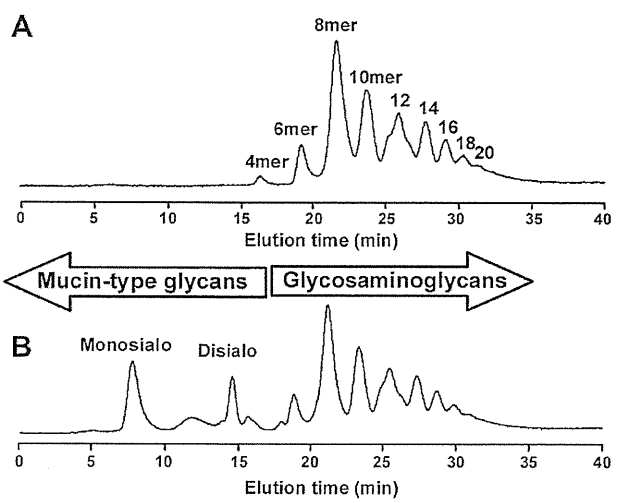

Fig.1. Separation of mucin-type glycans and GAGs by serotonin affinity chromatography. 2AA-labeled HA oligosaccharides (A) and a mixture of HA oligosaccharides and mucin-type glycans derived from bovine fetuin (B) are shown. Analytical conditions: eluent, water (solvent A) and 40 mM ammonium acetate (solvent B); gradient condition, linear gradient (5–75% solvent B) from 2 to 37 min and 75 to 100% solvent B from 37 to 45 min.

One-pot analysis of mucin-type glycans and GAGs from HCT116 cells

In the initial step of the analysis of *O*-glycans expressed on HCT116 cells, the released glycans were separated by serotonin affinity chromatography (Fig. 2). Asialo (M1), monosialo (M2 and M3) and disialo (M4–M6) mucin-type glycans were observed at 3–5, 5.2–10.0, and 10.8–16.0 min, respectively. After all mucin-type glycans were eluted, GAGs were eluted with 1 M NaCl. Each fraction obtained in this way was analyzed according to the method described in Materials and methods.

Six mucin-type glycan fractions (M1–M6) were analyzed by NP–HPLC and MALDI–TOF MS (Fig. 3), and the list of the observed mucin-type glycans in HCT116 cells is summarized in Table 1. The MS data were analyzed by Glycopeakfinder and Glycoworkbench in EUROCarbDB (http://www.ebi.ac.uk/eurocarb/tools.action). The amounts of expressed mucin-type glycans were calculated from the peak areas observed by NP–HPLC. We found 31 mucin-type glycans in HCT116 cells. Asialo glycans, T antigen (*m/z* 503: Galβ1-3GalNAc-2AA), core 2 structure (*m/z* 706: Galβ1-3(GlcNAcβ1-6)GalNAc-2AA), galactosyl core 2 structure (*m/z* 868: Galβ1-3(Galβ1-4GlcNAcβ1-6)GalNAc-2AA), and a polylactosamine-type glycan (*m/z* 1233: $Hex_3HexNAc_3$-2AA) were observed. Tandem MS (MS/MS) analysis of the peak observed at 1233 gave the ions at *m/z* 544 and 503 (Fig. 4A). These ions are obviously due to GlcNAcβ1-6GalNAc-2AA and Galβ1-3GalNAc-2AA (Fig. 4A). Based on these results, the glycan observed at *m/z* 1233 was confirmed as polylactosaminyl core 2 structure, Gal-GlcNAc-Galβ1-4 GlcNAcβ1-6(Galβ1-3)GalNAc-2AA. Monosialo core 1 and core 2 structures were found in monosialo glycan fractions (M2 and M3). Monosialo-polylactosamine-type glycans were also clearly observed in M2. These glycans have polylactosaminyl core 2 structure. Monosialo glycans having smaller molecular sizes such as sialyl-T and monosialo core 2 structure were observed in M3. Disialo core 1, core 2, and disialo-polylactosaminyl glycans were observed in M4, M5, and M6. It should be noted that mono sulfated mucin-type glycans were observed in HCT116 cells. The molecular ion at *m/z* 1604 observed in M6 is due to $NeuAc_1Hex_3HexNAc_3$-2AA + SO_3. After neuraminidase digestion, MS/MS analysis of this glycan afforded a desulfated molecular ion peak at *m/z* 1233 (Fig. 4B, upper spectrum). By MS^3 analysis, the fragment ion peak observed at *m/z* 1233 is confirmed as polylactosaminyl core 2 structure, Gal-GlcNAc-Galβ1–4 GlcNAcβ1-6(Galβ1-3)GalNAc-2AA (Fig. 4B, lower spectrum). In addition, two fragment ion peaks at *m/z* 444 and 948 were observed in MS^2 spectrum (Fig. 4B, upper spectrum). The fragment ion peak at *m/z* 444 corresponds to sulfated lactosamine, GalGlcNAc + SO_3. The fragment ion peak at *m/z*

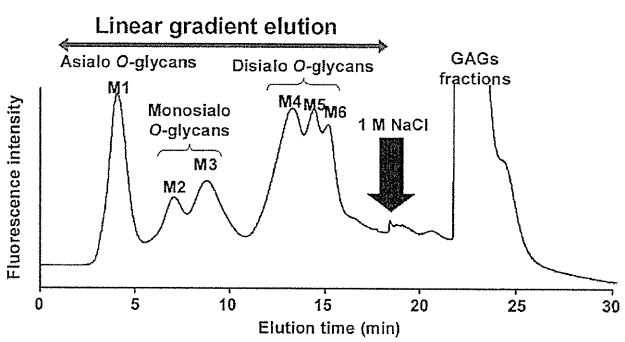

Fig.2. Separation of mucin-type glycans and GAGs derived from HCT116 cells by serotonin affinity chromatography. Analytical conditions: eluent, water (solvent A) and 40 mM ammonium acetate (solvent B); gradient condition, linear gradient (5–41% solvent B) from 2 to 20 min. After collecting the mucin-type glycans, GAGs were eluted with 1 M NaCl.

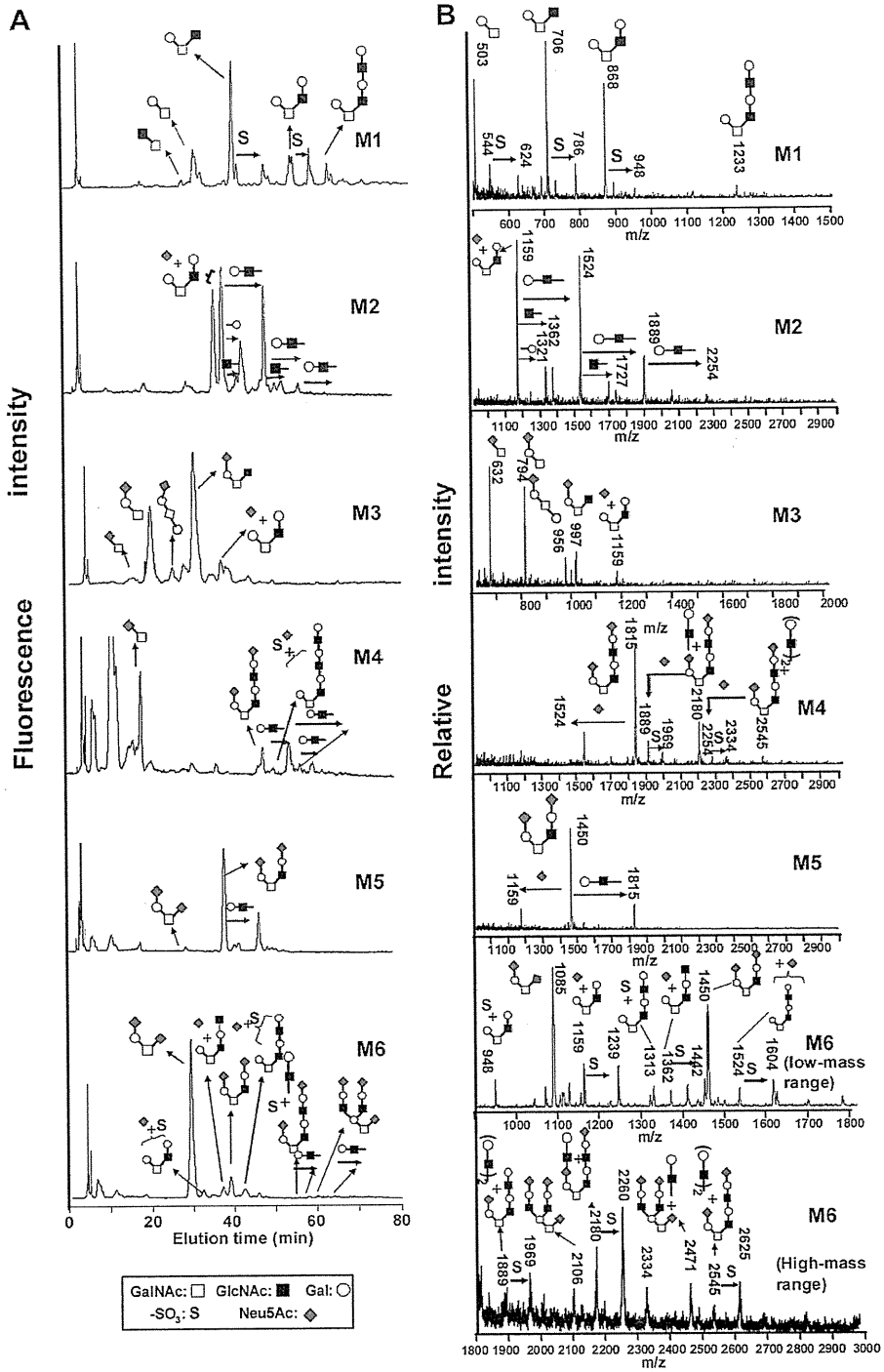

Fig.3. NP–HPLC and MALDI–TOF MS analysis of mucin-type glycans derived from HCT116 cells. The mucin-type glycan fractions separated by serotonin affinity chromatography were analyzed by NP–HPLC (A) and MALDI–TOF MS (B). Analytical conditions of HPLC: column, Amide-80 (Tosoh, 4.6 × 250 nm); solvent A, 0.1% CH_3COOH in acetonitrile; solvent B, 0.2% CH_3COOH–0.1% triethylamine in water; gradient condition, linear gradient (15–65% solvent B) from 2 to 82 min.

948 is due to sulfated galactosyl core 2 structure, Galβ1-4GlcNAcβ1-6(Galβ1-3)GalNAc-2AA + SO_3. This fragment ion indicates that terminal lactosamine is not sulfated. It was reported that GlcNAc-6-*O*-sulfotransferase was expressed and Gal-3-*O*-sulfotransferase was down-regulated in colon cancer cells [40]. Based on these considerations, we concluded that the structure of this sulfate-containing mucin-type glycan was Gal-GlcNAc-Galβ1-4(SO_3-6)GlcNAcβ1-6(Galβ1-3)GalNAc-2AA. These types of sulfated glycans were also observed in M1 and M4.

GAG fractions collected by serotonin affinity chromatography were analyzed as unsaturated disaccharides after digestion with specific eliminases. Half of the fractions were digested with chondroitinase ABC, and the other half were treated with a combination of heparitinases 1 and 2. The mixture of unsaturated disaccharides

Table 1
Mucin-type glycans found in HCT116 cells.

Structure	Observed molecular ion peaks (*m/z*)	Amount of glycans (pmol/L × 10^6 cells)
Asialo glycans		
Galβ1-3GalNAc-2AA	503	67.1
GlcNAcβ1-3GalNAc-2AA	544	0.5
Galβ1-3(GlcNAcβ1-6)GalNAc-2AA	706	142.1
Galβ1-3(Galβ1-4GlcNAcβ1-6)GalNAc-2AA	868	73.9
Galβ1-3(Gal-GlcNAc-Galβ1-4GlcNAcβ1-6)GalNAc-2AA	1233	41.8
Monosialo glycans		
NeuAcα2-6GalNAc-2AA	632	122.8
NeuAcα2-3Galβ1-3GalNAc-2AA	794	180.0
NeuAcα2-3Galβ1-3(GlcNAcβ1-6)GalNAc-2AA	997	294.3
Galβ1-3(Galβ1-4GlcNAcβ1-6)GalNAc-2AA + $NeuAc_1$	1159	191.7
Galβ1-3(GlcNAc-Galβ1-4GlcNAcβ1-6)GalNAc-2AA + $NeuAc_1$	1362	32.5
Galβ1-3(Gal-GlcNAc-Galβ1-4GlcNAcβ1-6)GalNAc-2AA + $NeuAc_1$	1524	120.7
Galβ1-3(GlcNAc-Gal-GlcNAc-Galβ1-4GlcNAcβ1-6)GalNAc-2AA + $NeuAc_1$	1727	34.3
Galβ1-3((Gal-GlcNAc)$_2$-Galβ1-4GlcNAcβ1-6)GalNAc-2AA + $NeuAc_1$	1889	32.8
Galβ1-3((Gal-GlcNAc)$_3$-Galβ1-4GlcNAcβ1-6)GalNAc-2AA + $NeuAc_1$	2254	21.5
Disialo glycans		
NeuAcα2-3Galβ1-3(NeuAcα2-6)GalNAc-2AA	1085	217.3
NeuAc-Galβ1-3(NeuAc-Galβ1-4GlcNAcβ1-6)GalNAc-2AA	1450	199.6
NeuAcα2-3Galβ1-3(NeuAc-Gal-GlcNAc-Galβ1-4GlcNAcβ1-6)GalNAc-2AA	1815	170.1
NeuAcα2-3Galβ1-3(NeuAc-(Gal-GlcNAc)$_2$-Galβ1-4GlcNAcβ1-6)GalNAc-2AA	2180	56.0
NeuAcα2-3Galβ1-3(NeuAc-(Gal-GlcNAc)$_3$-Galβ1-4GlcNAcβ1-6)GalNAc-2AA	2545	18.0
Trisialo glycans		
NeuAc-Gal-GlcNAc-(NeuAc-Gal-GlcNAc)Galβ1-3(NeuAcα2-6)GalNAc-2AA	2106	0.5
NeuAc-Gal-GlcNAc(NeuAc-Gal-GlcNAc)Galβ1-3(NeuAcα2-6)GalNAc-2AA + Gal-GlcNAc	2471	0.2
Sulfate glycans		
HexNAc-HexNAc-2AA + SO_3	624	2.3
Galβ1-3(GlcNAcβ1-6)GalNAc-2AA + SO_3	786	66.6
Galβ1-3(Galβ1-4GlcNAcβ1-6)GalNAc-2AA + SO_3	948	81.0
Galβ1-3(Galβ1-4GlcNAcβ1-6)GalNAc-2AA + NeuAc + SO_3	1239	8.8
Galβ1-3(GlcNAc-Galβ1-4GlcNAcβ1-6)GalNAc-2AA + NeuAc + SO_3	1442	17.7
Galβ1-3(Gal-GlcNAc-Galβ1-4GlcNAcβ1-6)GalNAc-2AA + $NeuAc_1$ + SO_3	1604	19.5
Galβ1-3((Gal-GlcNAc)$_2$-Galβ1-4GlcNAcβ1-6)GalNAc-2AA + $NeuAc_1$ + SO_3	1969	1.4
NeuAcα2-3Galβ1-3(NeuAc-(Gal-GlcNAc)$_2$-Galβ1-4GlcNAcβ1-6)GalNAc-2AA + SO_3	2260	3.2
Galβ1-3((Gal-GlcNAc)$_3$-Galβ1-4GlcNAcβ1-6)GalNAc-2AA + $NeuAc_1$ + SO_3	2334	0.2
NeuAcα2-3Galβ1-3(NeuAc-(Gal-GlcNAc)$_3$-Galβ1-4GlcNAcβ1-6)GalNAc-2AA + SO_3	2625	0.5

obtained in this way was labeled with 2AA and analyzed by laser-induced fluorescence (LIF)–CE (Fig. 5). Peaks were assigned by comparing the migration times with those of the standard unsaturated disaccharides. As shown in Fig. 5A (upper panel), we achieved excellent separation of nine unsaturated disaccharides from chondroitin sulfate (CS) and HA. We also succeeded in separation of seven unsaturated disaccharides from HS (Fig. 5B, upper panel). Five unsaturated disaccharides, ΔdiCS-diS_E (SE), ΔdiCS-6S (6S), ΔdiCS-4S (4S), ΔdiCS-0S (0S), and Δdi-HA (HA), were observed in the mixture after digestion with chondroitinase ABC (Fig. 5A, lower panel; see the list of the structures in Fig. 5A). Relative abundance of Δdi-HA was much higher than those of other unsaturated disaccharides in HCT116 cells. Seven unsaturated disaccharides, ΔdiHS-triS (TriS), ΔdiHS-diS3 (S3), ΔdiHS-diS2 (S2), ΔdiHS-diS1 (S1), ΔdiHS-6S (6S), ΔdiHS-NS (NS), and ΔdiHS-0S (0S), were observed in the mixture digested with a combination of heparitinases 1 and 2 (Fig. 5B, lower panel). Relative abundance of unsulfated HS disaccharide (HS0S) was much higher than those of other unsaturated disaccharides in HCT116 cells. It should be noted that there are no other contaminating peaks due to mucin-type *O*-glycans. From these results, it was revealed that mucin-type glycans as well as GAGs were able to be analyzed in the same sample.

Characterization of cancer cell lines

Based on the results obtained by the analysis of both mucin-type glycans and GAGs in HCT116 cells, we applied the methods to the analysis of both glycans on various cancer cells. The results are summarized in Figs. 6–8. Fig. 6 shows the total amount of mucin-type glycans and GAGs expressed on 10 cancer cell lines. The amounts of the expressed mucin-type glycans and GAGs were calculated from the peak areas observed by NP–HPLC and CE, respectively. There are significant differences in the expression levels of mucin-type glycans and GAGs among leukemia cells and epithelial cells. All leukemia cell lines poorly express both mucin-type glycans and GAGs. In contrast, epithelial cells express large amounts of them, although the amounts of the glycans are conspicuously varied among cell lines. There are 10–100 times larger amounts of mucin-type glycans than GAGs present on cancer cells. This is probably because proteoglycans are not present as conjugates in cell membrane but rather loosely interact with the components of cell surface. During the purification step of whole proteins, some portions of proteoglycans are not collected or the expression level of proteoglycans may be intrinsically lower than that of mucin-type glycans, although further studies are required. In any case, the data indicate that glycans are not dense on the floating blood cells. In contrast, glycans in epithelial cells, which form tumor tissues, are present in high density and seem to show important roles in exchanging intercellular information.

Figs. 7 and 8 show comparisons of relative abundances of mucin-type glycans and unsaturated disaccharides derived from glycosaminoglycans in cancer cells. Fig. 7 shows the glycan profiles obtained from four leukemia cells. All cell lines commonly contained sialyl-T and disialyl-T antigens as major mucin-type glycans. K562 and U937 cells especially contained these two glycans as the major glycans. Although it was difficult to discriminate these two cells only by mucin-type glycan analysis, profiling of GAGs

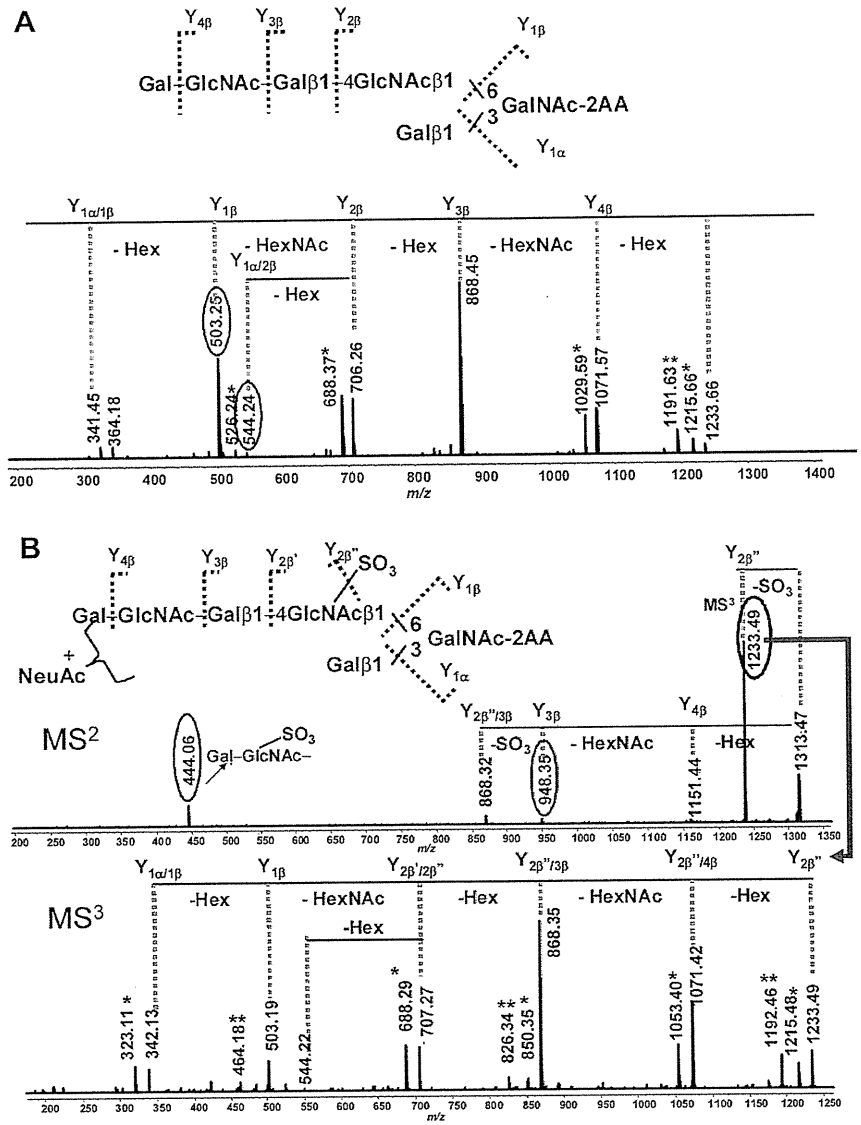

Fig.4. MS/MS analysis of mucin-type glycans derived from HCT116 cells. (A) Polylactosaminyl mucin-type glycan observed at *m/z* 1233. (B) Sulfated mucin-type glycan observed at *m/z* 1604.

could easily discriminate these cells. K562 cells contained ΔdiCS-4S as the major component. In contrast, ΔdiHS-0S was the major component in U937 cells. U937 cells also contained ΔdiCS-4S, but the relative abundance of this unsaturated disaccharide was low. Jurkat cells expressed extremely large amount of Tn antigen. GAGs in Jurkat cells showed profiles similar to those observed in U937 cells. HL-60 cells expressed core 2 mucin-type glycans abundantly. In addition, polylactosaminyl and fucosylated mucin-type glycans were also observed in HL-60 cells. A feature of HL-60 cells is that the cells express elongated mucin-type glycans in comparison with other leukemia cells. ΔdiCS-0S was the major component in HL-60 cells. This means that low-sulfated GAGs were abundant in HL-60 cells.

Fig. 8 shows the results on the characterization of six epithelial cancer cell lines. Mucin-type glycan profiles in epithelial cancer cell lines except PANC1 cells are generally more complex than those of leukemia cancer cells. This means that characterization of mucin-type glycans on epithelial cancer cells will be a powerful tool for correlating with their biological characteristics such as tumorigenesis ability. Sialyl-T and disialyl-T antigens were commonly observed in all cancer cells, although their relative abundances were diverse among cells. However, all cancer cells scarcely expressed core 3 and core 4 structures. These data are well correlated with the reports on down-regulation of these glycans in various tumor tissues [21,22]. Profiles of GAGs also gave interesting results. Relative abundances of HA in epithelial cancer cells were commonly higher than those in leukemia cells. In addition, relative abundances of ΔdiHS-0S also showed higher values than those observed for leukemia cells. These data indicate that sulfation level of HS is significantly low in cancer cell lines. Recently, some research groups reported that HS sulfatases (SULF) are overexpressed in subsets of multiple tumors [41–43]. SULF2 overexpressed in tumor tissues was associated with tumor prognosis [42,44]. These reports indicate that sulfation level of HS is decreased in certain cancer cell lines. Our results are well correlated with these observations. PANC1 cells (poorly differentiated pancreatic cancer cells) expressed sialyl-T and disialyl-T as the major mucin-type glycans. The elongated mucin-type glycans were not

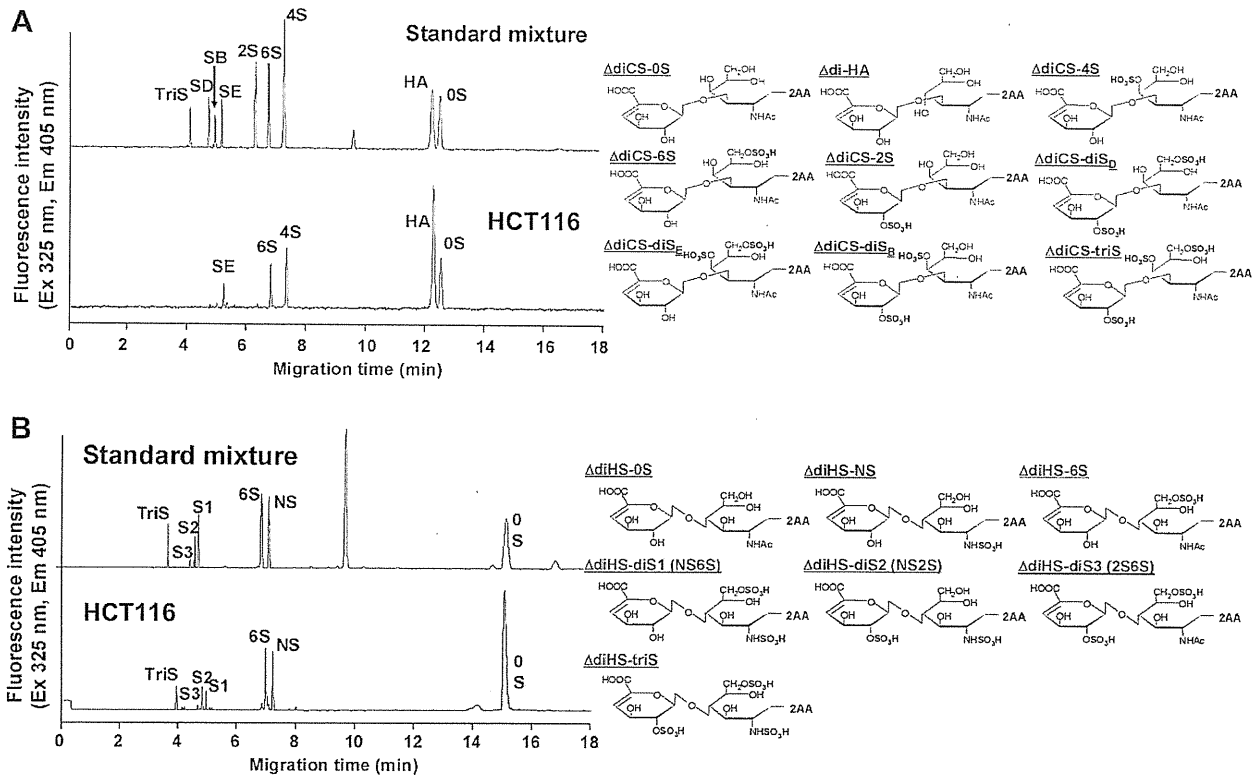

Fig.5. Analysis of unsaturated disaccharides from GAG fractions. 2AA-labeled unsaturated disaccharides of HA and CS (A) and of HS (B) in HCT116 cells were analyzed by CE. Analytical conditions: capillary, fused silica (40 cm × 50 μm i.d); running buffer, 100 mM Tris–phosphate (pH 3.0); applied voltage, 25 kV; injection, pressure method (1.0 psi for 10 s); temperature, 25 °C; detection, He-Cd laser-induced fluorescent detection (excitation 325 nm, emission 405 nm). Abbreviations of unsaturated disaccharide: (A) Unsaturated chondroitin and hyaluronic acid disaccharide: 0S, ΔdiCS-0S (12.8 min); HA, ΔdiHA (12.3 min); 4S, ΔdiCS-4S (7.4 min); 6S, ΔdiCS-6S (6.8 min); 2S, ΔdiCS-2S (6.5 min); SD, ΔdiCS-diS$_D$ (4.8 min); SE, ΔdiCS-diS$_E$ (5.2 min); SB, ΔdiCS-diS$_B$ (5.0 min); TriS, ΔdiCS-triS (4.1 min). (B) Unsaturated heparan sulfate disaccharide: 0S, ΔdiHS-0S (15.3 min); NS, ΔdiHS-NS (7.2 min); 6S, ΔdiHS-6S (6.8 min); S1, ΔdiHS-diS1 (5.0 min); S2, ΔdiHS-diS2 (4.9 min); S3, ΔdiHS-diS3 (4.8 min); TriS, ΔdiHS-TriS (4.0 min).

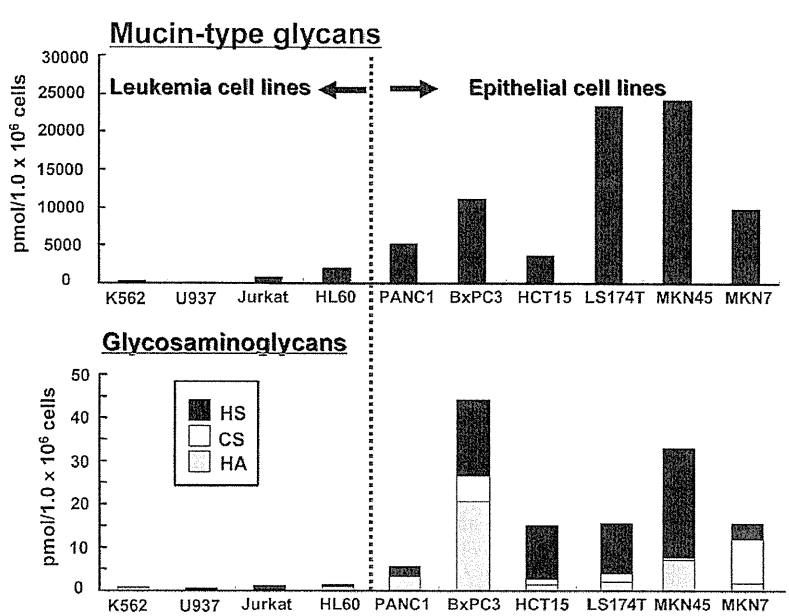

Fig.6. Comparison of the amounts of mucin-type glycans and GAGs expressed on cancer cells. The amounts of the expressed mucin-type glycans and GAGs were calculated from the peak areas observed by NP–HPLC and CE, respectively.

observed in PANC1 cells. Because PANC1 cells lack core 2 β-1,6-*N*-acetylglucosaminyltransferase, which is required for elongation of the mucin-type glycans [45], these observations suggest that tumor-associated epitopes on mucin core proteins expressed on

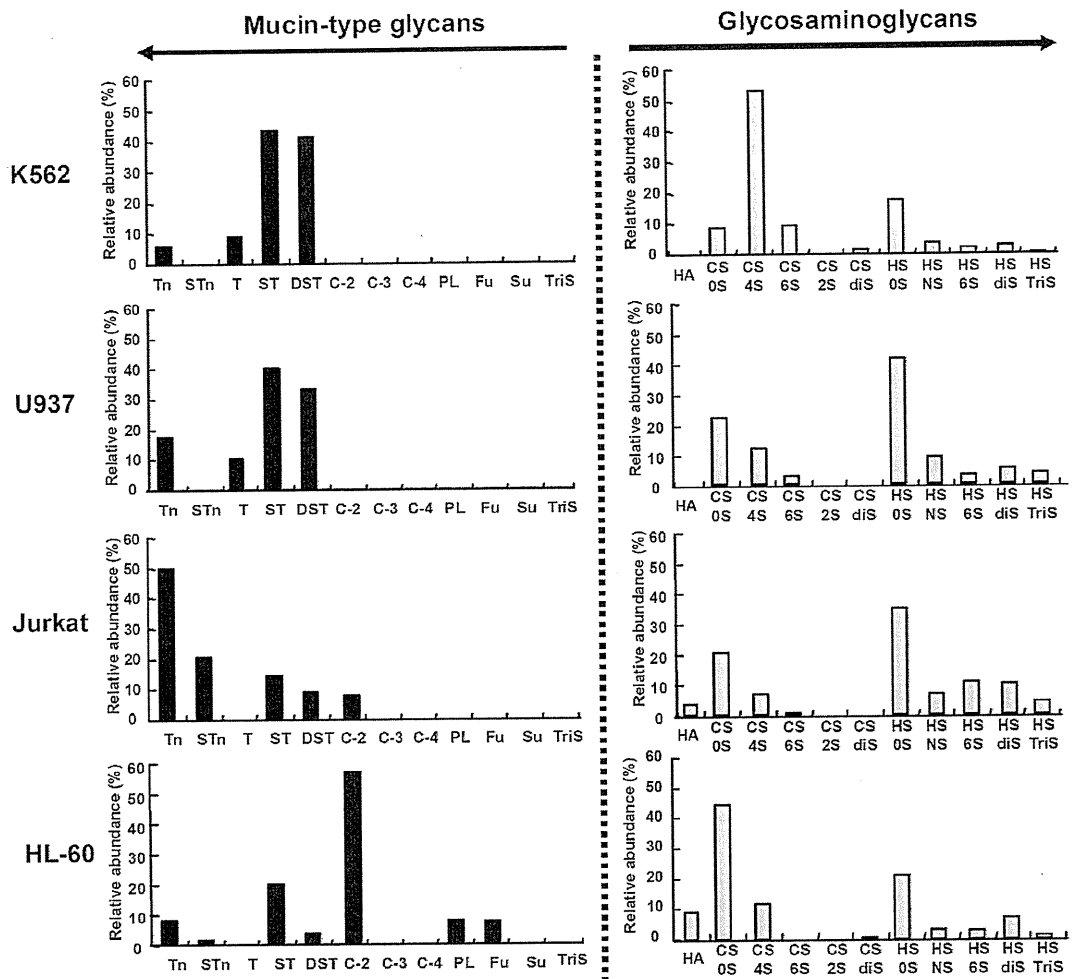

Fig.7. Characterization of four leukemia cell lines. The contents of mucin-type glycans and GAGs are displayed as black bars and gray bars, respectively. Relative abundances of mucin-type glycans and unsaturated disaccharides were calculated from the peak areas observed by NP–HPLC and CE, respectively. Abbreviations: Tn, Tn antigen; STn, sialyl-Tn antigen; T, T antigen; ST, sialyl-T antigen; DST, disialyl-T antigen; C-2, core 2 structure; C-3, core 3 structure; C-4, core 4 structure; PL, polylactosamine-type structure; Fu, fucosylated structure; Su, sulfated structure; TriS, trisialylated structure; HA, Δdi-HA; CS-0S, ΔdiCS-0S; CS-4S, ΔdiCS-4S; CS-6S, ΔdiCS-6S; CS-2S, ΔdiCS-2S; CS-diS, disulfated unsaturated disaccharides of CS; HS-0S, ΔdiHS-0S; HS-NS, ΔdiHS-NS; HS-6S, ΔdiHS-6S; HS-diS, disulfated unsaturated disaccharides of HS; HS-TriS, trisulfated unsaturated disaccharides of HS.

PANC1 cells are exposed to the external environment. Mucin-type glycans of BxPC3 cells were obviously different from those of PANC1 cells. Core 2 structure was the major glycan in BxPC3 cells, and its modified structures (i.e., polylactosaminyl structure and fucosylated glycans) were also observed in BxPC3 cells. Mare and Trinchera reported that BxPC3 cells expressed polylactosamine-type glycans [46]. The profiles of GAGs of PANC1 cells are quite interesting, and only HA and low-sulfated HS (HS0S) were observed. HA and HS were also the major GAGs in BxPC3 cells (moderately differentiated pancreatic cancer cell lines), and profiles similar to those of PANC1 cells were reported. The expression level of HA was increased in pancreatic cancer cells [35], and its increase was a risk factor for tumor proliferation and metastasis [36,47]. In addition, BxPC3 cells obviously expressed CS, which was not observed in PANC1 cells. Sulfated mucin-type glycans were characteristically observed in colon cancer cell lines, HCT15 and LS174T. HCT15 cells expressed core 2 and polylactosamine-type glycans as the major mucin-type glycans. In addition, sialyl-T and disialyl-T were abundant in HCT15 cells. Most of the abundant mucin-type glycans in LS174T cells were fucosylated. LS174T cells also expressed large amounts of Tn antigen and polylactosamine-type glycans. This is a specific feature of LS174T cells in which both truncated and extended glycans were present. Both HCT15 and LS174T cells contained low-sulfated HS (HS0S) as the major GAGs. In contrast, the level of HS sulfation in HCT15 cells was a little bit higher than that observed in LS174T cells. However, relative abundance of ΔdiCS-6S in LS174T cells was higher than that in HCT15 cells. We previously reported that the profiles of mucin-type glycans were dramatically changed with differentiation stages of gastric cancer cell lines [38]. Poorly differentiated gastric cancer cells (MKN45 cells) expressed large amounts of extended polylactosamine-type glycans with molecular masses greater than 6000 [38]. In addition, trisialylated mucin-type glycans were characteristically observed in MKN45 cells. In contrast, polylactosamine-type glycans were not observed in well-differentiated gastric cancer cells (MKN7 cells). In MKN7 cells, glycans of core 2 structure were observed abundantly. This means that elongation of core 2 structure to polylactosamine-type glycan is suppressed in MKN7 cells, although further studies on the related synthetic enzymes are required. Profiles of GAGs in these two gastric cancer cells were quite different. HA and low-sulfated HS (HS0S) were abundant, but CSs were scarcely observed in MKN45 cells. In contrast, CSs were the major GAGs in MKN7 cells. Relative abundance of ΔdiCS-4S was especially distinct in MKN7 cells.

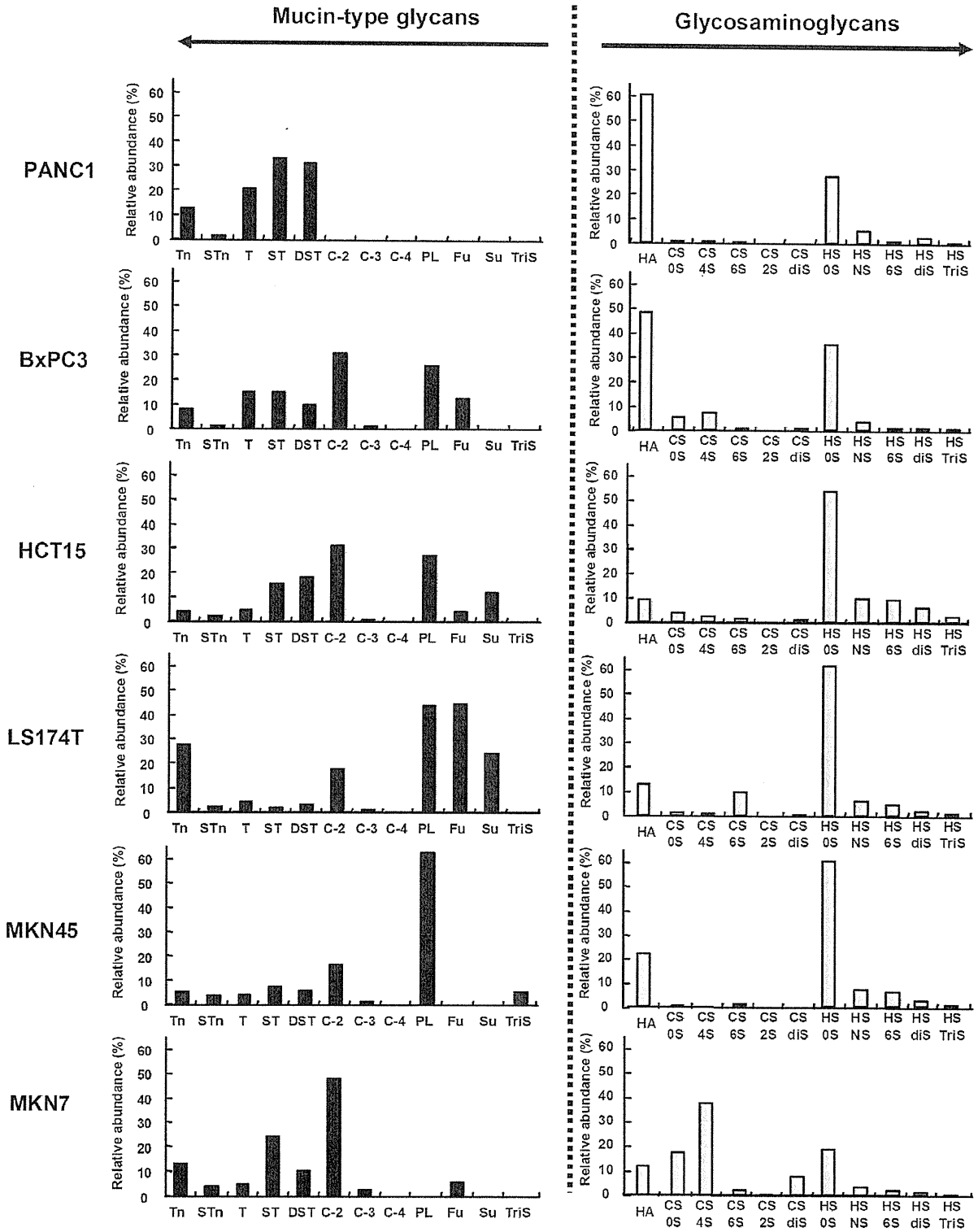

Fig.8. Characterization of six epithelial cancer cell lines. The contents of mucin-type glycans and GAGs are displayed as black bars and gray bars, respectively. Calculation of relative abundances and abbreviations are the same as in Fig. 7.

Although further studies are required, these results may indicate that GAGs play an important role in differentiation of gastric cancer cells.

As described above, it was revealed that our methods are useful to characterize the various cancer cell lines. In the future, we will apply these methods to compare *O*-glycan profiles between cancer

cells and normal cells and to reveal the tumor-specific alterations of *O*-glycan profiles.

Conclusion

We have developed an automatic system for releasing *O*-glycans from glycoproteins and applied the methods to the analysis of the released mucin-type glycans. In the current study, we developed methods for one-pot analysis of mucin-type glycans and GAGs. Serotonin affinity chromatography for group separation of mucin-type glycans based on the number of sialic acid residues [38] is also useful for collection of GAGs. As shown in Fig. 1, GAGs were strongly retained on the serotonin-immobilized column, and group separation of GAGs and mucin-type glycans was easily achieved. After collection of these glycans, mucin-type glycans were conveniently analyzed by MALDI–TOF MS and HPLC, and GAGs could be analyzed by CE as a mixture of unsaturated disaccharides after digestion with specific eliminases.

Two leukemia cancer cell lines (U937 and K562) showed similar profiles of mucin-type glycans and could not be discriminated only by comparing mucin-type glycans. However, GAG profiles showed obviously distinct characteristics (Fig. 7). In contrast, pancreatic cancer cell lines (PANC1 and BxPC3) showed similar GAG profiles but quite different mucin-type glycan profiles (Fig. 8). We also revealed that the profiles of GAGs as well as mucin-type glycans were dramatically altered at different differentiation stages of cancer cells, as determined by the analysis of MKN45 and MKN7 cells.

Based on these results, the current techniques will be useful to discover the novel biomarkers for diseases. However, the relationship between biological characteristics and *O*-glycan profiles observed in cancer cells might not be the same with that observed in actual physiological conditions. Therefore, to discover the practical glycan biomarkers for diagnosis of tumors, our method needs to be applied to the clinical samples such as serum or tissue samples. We are now applying the current methods to various kinds of biological samples. Furthermore, we are also developing methods for identification of proteins carrying specific glycans. These results will be shown in future publications.

Appendix A. Supplementary data

Supplementary data associated with this article can be found, in the online version, at doi:10.1016/j.ab.2011.12.017.

References

[1] S. Kamoda, M. Nakano, R. Ishikawa, S. Suzuki, K. Kakehi, Rapid and sensitive screening of *N*-glycans as 9-fluorenylmethyl derivatives by high-performance liquid chromatography: a method which can recover free oligosaccharides after analysis, J. Proteome Res. 4 (2005) 146–152.

[2] R. Naka, S. Kamoda, A. Ishizuka, M. Kinoshita, K. Kakehi, Analysis of total *N*-glycans in cell membrane fractions of cancer cells using a combination of serotonin affinity chromatography and normal phase chromatography, J. Proteome Res. 5 (2006) 88–97.

[3] S. Kamoda, R. Ishikawa, K. Kakehi, Capillary electrophoresis with laser-induced fluorescence detection for detailed studies on N-linked oligosaccharide profile of therapeutic recombinant monoclonal antibodies, J. Chromatogr. A 1133 (2006) 332–339.

[4] K. Kakehi, A. Susami, A. Taga, S. Suzuki, S. Honda, High-performance capillary electrophoresis of O-glycosidically linked sialic acid-containing oligosaccharides in glycoproteins as their alditol derivatives with low-wavelength UV monitoring, J. Chromatogr. A 680 (1994) 209–215.

[5] B.L. Schulz, N.H. Packer, N.G. Karlsson, Small-scale analysis of O-linked oligosaccharides from glycoproteins and mucins separated by gel electrophoresis, Anal. Chem. 74 (2002) 6088–6097.

[6] M. Backstrom, K.A. Thomsson, H. Karlsson, G.C. Hansson, Sensitive liquid chromatography–electrospray mass spectrometry allows for the analysis of the O-glycosylation of immunoprecipitated proteins from cells or tissues: application to MUC1 glycosylation in cancer, J. Proteome Res. 8 (2009) 538–545.

[7] L. Royle, T.S. Mattu, E. Hart, J.I. Langridge, A.H. Merry, N. Murphy, D.J. Harvey, R.A. Dwek, P.M. Rudd, An analytical and structural database provides a strategy for sequencing *O*-glycans from microgram quantities of glycoproteins, Anal. Biochem. 304 (2002) 70–90.

[8] Y. Huang, Y. Mechref, M.V. Novotny, Microscale nonreductive release of O-linked glycans for subsequent analysis through MALDI mass spectrometry and capillary electrophoresis, Anal. Chem. 73 (2001) 6063–6069.

[9] K. Yamada, S. Hyodo, Y.K. Matsuno, M. Kinoshita, S.Z. Maruyama, Y.S. Osaka, E. Casal, Y.C. Lee, K. Kakehi, Rapid and sensitive analysis of mucin-type glycans using an in-line flow glycan-releasing apparatus, Anal. Biochem. 371 (2007) 52–61.

[10] K. Yamada, K. Kakehi, Recent advances in the analysis of carbohydrates for biomedical use, J. Pharm. Biomed. Anal. 55 (2011) 702–727.

[11] K. Yamada, S. Hyodo, M. Kinoshita, T. Hayakawa, K. Kakehi, Hyphenated technique for releasing and MALDI MS analysis of *O*-glycans in mucin-type glycoprotein samples, Anal. Chem. 82 (2010) 7436–7443.

[12] Y.K. Matsuno, K. Yamada, A. Tanabe, M. Kinoshita, S.Z. Maruyama, Y.S. Osaka, T. Masuko, K. Kakehi, Development of an apparatus for rapid release of oligosaccharides at the glycosaminoglycan–protein linkage region in chondroitin sulfate-type proteoglycans, Anal. Biochem. 362 (2007) 245–257.

[13] R.S. Aquino, E.S. Lee, P.W. Park, Diverse functions of glycosaminoglycans in infectious diseases, Prog. Mol. Biol. Transl. Sci. 93 (2010) 373–394.

[14] S. Mizuguchi, T. Uyama, H. Kitagawa, K.H. Nomura, K. Dejima, K. Gengyo-Ando, S. Mitani, K. Sugahara, K. Nomura, Chondroitin proteoglycans are involved in cell division of *Caenorhabditis elegans*, Nature 423 (2003) 443–448.

[15] A. Guzman-Aranguez, P. Argueso, Structure and biological roles of mucin-type *O*-glycans at the ocular surface, Ocul. Surf. 8 (2010) 8–17.

[16] N.L. Perillo, K.E. Pace, J.J. Seilhamer, L.G. Baum, Apoptosis of T cells mediated by galectin-1, Nature 378 (1995) 736–739.

[17] S.J. Storr, L. Royle, C.J. Chapman, U.M. Hamid, J.F. Robertson, A. Murray, R.A. Dwek, P.M. Rudd, The O-linked glycosylation of secretory/shed MUC1 from an advanced breast cancer patient's serum, Glycobiology 18 (2008) 456–462.

[18] P.H. Jensen, D. Kolarich, N.H. Packer, Mucin-type O-glycosylation – putting the pieces together, FEBS J. 277 (2010) 81–94.

[19] Y. Mechref, M.V. Novotny, Structural investigations of glycoconjugates at high sensitivity, Chem. Rev. 102 (2002) 321–369.

[20] H.J. An, S.R. Kronewitter, M.L. de Leoz, C.B. Lebrilla, Glycomics and disease markers, Curr. Opin. Chem. Biol. 13 (2009) 601–607.

[21] S.H. Lee, M. Fukuda, Core 3 glycan as tumor suppressor, Methods Enzymol. 479 (2010) 143–154.

[22] T. Iwai, T. Kudo, R. Kawamoto, T. Kubota, A. Togayachi, T. Hiruma, T. Okada, T. Kawamoto, K. Morozumi, H. Narimatsu, Core 3 synthase is down-regulated in colon carcinoma and profoundly suppresses the metastatic potential of carcinoma cells, Proc. Natl Acad. Sci. USA 102 (2005) 4572–4577.

[23] I. Brockhausen, Pathways of *O*-glycan biosynthesis in cancer cells, Biochim. Biophys. Acta 1473 (1999) 67–95.

[24] I. Brockhausen, Sulphotransferases acting on mucin-type oligosaccharides, Biochem. Soc. Trans. 31 (2003) 318–325.

[25] I. Brockhausen, Glycodynamics of mucin biosynthesis in gastrointestinal tumor cells, Adv. Exp. Med. Biol. 535 (2003) 163–188.

[26] G.F. Springer, T and Tn, general carcinoma autoantigens, Science 224 (1984) 1198–1206.

[27] S. Nakamori, M. Kameyama, S. Imaoka, H. Furukawa, O. Ishikawa, Y. Sasaki, T. Kabuto, T. Iwanaga, Y. Matsushita, T. Irimura, Increased expression of sialyl Lewis^x antigen correlates with poor survival in patients with colorectal carcinoma: clinicopathological and immunohistochemical study, Cancer Res. 53 (1993) 3632–3637.

[28] C. Hanski, E. Klussmann, J. Wang, C. Bohm, D. Ogorek, M.L. Hanski, S. Kruger-Krasagakes, J. Eberle, A. Schmitt-Graff, E.O. Riecken, Fucosyltransferase III and sialyl-Le^x expression correlate in cultured colon carcinoma cells but not in colon carcinoma tissue, Glycoconj. J. 13 (1996) 727–733.

[29] N. Kojima, K. Handa, W. Newman, S. Hakomori, Inhibition of selectin-dependent tumor cell adhesion to endothelial cells and platelets by blocking O-glycosylation of these cells, Biochem. Biophys. Res. Commun. 182 (1992) 1288–1295.

[30] Y.H. Teng, P.H. Tan, S.J. Chia, N.A. Zam, W.K. Lau, C.W. Cheng, B.H. Bay, G.W. Yip, Increased expression of non-sulfated chondroitin correlates with adverse clinicopathological parameters in prostate cancer, Mod. Pathol. 21 (2008) 893–901.

[31] H. Nakanishi, K. Oguri, K. Yoshida, N. Itano, K. Takenaga, T. Kazama, A. Yoshida, M. Okayama, Structural differences between heparan sulphates of proteoglycan involved in the formation of basement membranes in vivo by Lewis-lung-carcinoma-derived cloned cells with different metastatic potentials, Biochem. J. 288 (1992) 215–224.

[32] K. Raman, B. Kuberan, Chemical tumor biology of heparan sulfate proteoglycans, Curr. Chem. Biol. 4 (2010) 20–31.

[33] R.D. Sanderson, Y. Yang, T. Kelly, V. MacLeod, Y. Dai, A. Theus, Enzymatic remodeling of heparan sulfate proteoglycans within the tumor microenvironment: Growth regulation and the prospect of new cancer therapies, J. Cell. Biochem. 96 (2005) 897–905.

[34] R. Sasisekharan, S. Ernst, G. Venkataraman, On the regulation of fibroblast growth factor activity by heparin-like glycosaminoglycans, Angiogenesis 1 (1997) 45–54.

[35] A.D. Theocharis, M.E. Tsara, N. Papageorgacopoulou, D.D. Karavias, D.A. Theocharis, Pancreatic carcinoma is characterized by elevated content of

hyaluronan and chondroitin sulfate with altered disaccharide composition, Biochim. Biophys. Acta 1502 (2000) 201–206.
[36] H. Morohashi, A. Kon, M. Nakai, M. Yamaguchi, I. Kakizaki, S. Yoshihara, M. Sasaki, K. Takagaki, Study of hyaluronan synthase inhibitor, 4-methylumbelliferone derivatives, on human pancreatic cancer cell (KP1-NL), Biochem. Biophys. Res. Commun. 345 (2006) 1454–1459.
[37] F.J. Vizoso, J.M. del Casar, M.D. Corte, I. Garcia, M.G. Corte, A. Alvarez, J.L. Garcia-Muniz, Significance of cytosolic hyaluronan levels in gastric cancer, Eur. J. Surg. Oncol. 30 (2004) 318–324.
[38] K. Yamada, M. Kinoshita, T. Hayakawa, S. Nakaya, K. Kakehi, Comparative studies on the structural features of *O*-glycans between leukemia and epithelial cell lines, J. Proteome Res. 8 (2009) 521–537.
[39] A. Ishizuka, Y. Hashimto, R. Naka, M. Kinoshita, K. Kakehi, J. Seino, Y. Funakoshi, T. Suzuki, A. Kameyama, H. Narimatsu, Accumulation of free complex-type *N*-glycans in MKN7 and MKN45 stomach cancer cells, Biochem. J. 413 (2008) 227–237.
[40] A. Seko, K. Nagata, S. Yonezawa, K. Yamashita, Ectopic expression of a GlcNAc 6-*O*-sulfotransferase, GlcNAc6ST-2, in colonic mucinous adenocarcinoma, Glycobiology 12 (2002) 379–388.
[41] N.P. Castro, C.A. Osorio, C. Torres, E.P. Bastos, M. Mourao-Neto, F.A. Soares, H.P. Brentani, D.M. Carraro, Evidence that molecular changes in cells occur before morphological alterations during the progression of breast ductal carcinoma, Breast Cancer Res. 10 (2008) R87.
[42] J.P. Lai, D.S. Sandhu, C. Yu, T. Han, C.D. Moser, K.K. Jackson, R.B. Guerrero, I. Aderca, H. Isomoto, M.M. Garrity-Park, H. Zou, A.M. Shire, D.M. Nagorney, S.O. Sanderson, A.A. Adjei, J.S. Lee, S.S. Thorgeirsson, L.R. Roberts, Sulfatase 2 up-regulates glypican 3, promotes fibroblast growth factor signaling, and decreases survival in hepatocellular carcinoma, Hepatology 47 (2008) 1211–1222.
[43] Y. Kudo, I. Ogawa, S. Kitajima, M. Kitagawa, H. Kawai, P.M. Gaffney, M. Miyauchi, T. Takata, Periostin promotes invasion and anchorage-independent growth in the metastatic process of head and neck cancer, Cancer Res. 66 (2006) 6928–6935.
[44] H. Lemjabbar-Alaoui, A. van Zante, M.S. Singer, Q. Xue, Y.Q. Wang, D. Tsay, B. He, D.M. Jablons, S.D. Rosen, Sulf-2, a heparan sulfate endosulfatase, promotes human lung carcinogenesis, Oncogene 29 (2010) 635–646.
[45] P.V. Beum, J. Singh, M. Burdick, M.A. Hollingsworth, P.W. Cheng, Expression of core 2β-1,6-*N*-acetylglucosaminyltransferase in a human pancreatic cancer cell line results in altered expression of MUC1 tumor-associated epitopes, J. Biol. Chem. 274 (1999) 24641–24648.
[46] L. Mare, M. Trinchera, Suppression of β-1,3-galactosyltransferase β-3Gal-T5 in cancer cells reduces sialyl-Lewis^a and enhances poly-*N*-acetyllactosamines and sialyl-Lewis^x on *O*-glycans, Eur. J. Biochem. 271 (2004) 186–194.
[47] C. Pellizzaro, A. Speranza, S. Zorzet, I. Crucil, G. Sava, I. Scarlata, S. Cantoni, M. Fedeli, D. Coradini, Inhibition of human pancreatic cell line MIA PaCa2 proliferation by HA-But, a hyaluronic butyric ester: a preliminary report, Pancreas 36 (2008) e15–e23.

Journal of Chromatography A, 1246 (2012) 84–89

Contents lists available at SciVerse ScienceDirect

Journal of Chromatography A

journal homepage: www.elsevier.com/locate/chroma

Partial filling affinity capillary electrophoresis using large-volume sample stacking with an electroosmotic flow pump for sensitive profiling of glycoprotein-derived oligosaccharides

Eriko Fukushima[a], Yuki Yagi[b], Sachio Yamamoto[a], Yumi Nakatani[a], Kazuaki Kakehi[a], Takao Hayakawa[a], Shigeo Suzuki[a,*]

[a] Faculty of Pharmaceutical Sciences, Kinki University, 3-4-1 Kowakae, Higashi-osaka, Osaka Japan[1]
[b] Kyowa Hakko Kirin Co., Ltd., 100-1, Hagiwara-machi, Takasaki, Gunma 370-0013, Japan[2]

ARTICLE INFO

Article history:
Available online 28 February 2012

Keywords:
Large-volume sample stacking with an electroosmotic flow pump
Partial filling affinity capillary electrophoresis
Glycoprotein-derived oligosaccharides

ABSTRACT

An online preconcentration technique, large-volume sample stacking with an electroosmotic flow pump (LVSEP) was combined with partial filling affinity capillary electrophoresis (PFACE) to realize highly sensitive analysis of the interaction of glycoprotein-derived oligosaccharides with some plant lectins. Oligosaccharides derivatized with 8-aminopyrene-1,3,6-trisulfonic acid (APTS) were delivered to an entire neutrally-coated capillary and then lectin solution was hydrodynamically introduced from the outlet of the capillary as a short plug. A negative voltage was then applied after immersion of both ends of the capillary in 100 mM Tris–acetate buffer, pH 7.0 containing 0.5% hydroxypropylcellulose as electrophoresis buffers. A low concentration of electrolytes in the sample solution causes a significant flow by electroendosmosis from anode to cathode and the APTS-labeled oligosaccharides move quickly towards the anode and concentrate in the lectin phase. Finally, electroosmotic flow becomes negligible when the capillary is filled with the background electrolyte delivered from the anodic reservoir and APTS-labeled saccharides pass through the lectin plug and are detected at the anodic end. If the APTS-labeled oligosaccharides are recognized by the lectin, the migration profiles should be altered. The sensitivity was enhanced by a factor of *ca.* 900 compared to typical hydrodynamic injection (3.45 kPa, 10 s). By this method, increased residence time of APTS-saccharides in the lectin plug indicates highly efficient interaction with lectins, which differs completely from the results obtained by ordinary lectin PFACE. The run-to-run repeatability ($n = 18$) of the migration time and peak area was high, with relative standard deviations of less than 0.7% and 6.1%, respectively.

1. Introduction

Glycosylation of proteins is a typical post-translational modification resulting from the covalent bonding of oligosaccharide chains by the concerted actions of glycosyltransferases and glycosidases, which creates several populations of glycans that may control the diverse functions of proteins [1]. Some of these play a pivotal role in many biological processes [2], including protein folding [3,4], physicochemical stability [5,6], immune response [7–12], and inflammation [13]. Understanding the function of oligosaccharide chains and their changes in relation to diseases has been complicated to date by challenges associated with their analysis and characterization [14]. Occupancy of a glycosylation site and the particular carbohydrate sequences and linkages at each site can vary considerably and contribute to heterogeneity. The structural complexity and diversity of saccharide chains complicates comprehensive understanding of glycosylation, which is only possible by high-resolution and sensitive analytical methods and techniques.

Technologies based on liquid chromatography–mass spectrometry (LC–MS) enable high-throughput analysis of glycan sequencing and have become the main methods feasible for elucidating the population of oligosaccharides in detail [15–19]. However, the diversity of glycosylation due to branching, linkage positions and differences in component monosaccharides (*e.g.*, mannose or galactose, glucosamine or galactosamine) is concealed by these methods. In addition, the sensitivity in MS strongly depends on molecular size, charge and hydrophobicity but most oligosaccharides are

* Corresponding author.
E-mail addresses: boo.0907@gmail.com (E. Fukushima), yuuki.yagi@kyowa-kirin.co.jp (Y. Yagi), sachio.yamamoto@gmail.com (S. Yamamoto), 0711610103d@kindai.ac.jp (Y. Nakatani), k.kakehi@phar.kindai.ac.jp (K. Kakehi), hayakawatakao@gmail.com (T. Hayakawa), suzuki@phar.kindai.ac.jp (S. Suzuki).
[1] Tel.: +81 6 6721 2332; fax: +81 6 6721 2353.
[2] Tel.: +81 27 353 7452; fax: +81 27 352 4977.

0021-9673/$ – see front matter © 2012 Elsevier B.V. All rights reserved.
doi:10.1016/j.chroma.2012.02.052

neutral, of high-molecular mass and are highly hydrophilic. Therefore, the MS sensitivity for oligosaccharides or glycopeptides is not very high. Moreover, coelution of other low molecular mass and hydrophobic compounds makes it difficult to obtain quantitative profiles of oligosaccharides. Therefore, the analysis of oligosaccharide chains following labeling with fluorescent tags is still important in glycosylation analysis.

Lectins are proteins of non-immune origin that interact specifically with carbohydrates without modifying them [20]. Most lectins bind primarily to monosaccharides but they bind to specific sequences of oligosaccharides with higher affinity and specificity. High specificity of lectins against certain oligosaccharides is helpful for profiling in glycoproteomics analysis [21]. Capillary electrophoresis (CE) analyses of oligosaccharides using lectins as affinity ligands have been studied by several authors [22–25]. The difference in migration profiles in the presence and absence of a lectin in the electrophoresis buffer indicates the presence of a specific sequence in the oligosaccharides, which enables the profiling of oligosaccharides in some glycoproteins. However, the wide variety of molecular distribution of glycans often causes difficulty due to the limits of detection.

To realize a highly sensitive analysis and to enhance the affinity interaction with a simple injection scheme in CE, we focused on the large-volume sample stacking with an electroosmotic pump (LVSEP) method as an online sample concentration technique [26–33]. This exhibits efficient preconcentration and separation performance and the sample components are stacked at the sample/buffer boundary for a long time. Therefore, by injecting lectin from the anodic end as a short plug followed by injection of sample solution to the entire capillary, anionic derivatives of oligosaccharides are continuously moved and stacked in the lectin plug until the completion of preconcentration.

In the present study, we evaluated the combination of the LVSEP and partial filling affinity capillary electrophoresis (PFACE) techniques as an alternative to the previously reported affinity CE using lectins, and compared the sensitivity, repeatability and the efficiency of affinity interaction.

2. Materials and methods

2.1. Chemicals

8-Aminopylene-1,3,6-trisulfonic acid (APTS), porcine thyroglobulin, human transferrin and immunoglobulin were obtained from Sigma–Aldrich Japan K.K. (Tokyo, Japan). *Aleuria aurantia* lectin (AAL), concanavalin A (Con A), *Erythrina cristagalli* lectin (ECA), *Maachia amurensis* mitogen (MAM), and *Sambucus sieboldiana* agglutinin (SSA) were obtained from Seikagaku Corporation (Tokyo, Japan). Peptide-N^4-(*N*-acetyl-β-glucosaminyl) asparagine amidase F (PNGase F, E.C. 3.5.1.52) was from Roche Applied Science (Tokyo, Japan). Neuraminidase (*Arthrobacter urefaciens)* was from Nacalai Tesque (Tokyo, Japan). Sodium cyanoborohydride and iodoacetamide were obtained from Wako Pure Chemical Industries Limited (Osaka, Japan). Biomimetic polymer surfactant (N102) solution from NOF Corporation (Tokyo, Japan) was used as received to coat the inner wall of the capillary. Other reagents and solvents were of the highest commercial grade. APTS-labeled oligosaccharides were prepared from glycoproteins as described previously [25].

2.2. LVSEP-PFACE Analysis of APTS-labeled oligosaccharides

In all CE separations, polydimethylsiloxane (PDMS)-coated capillaries (InertCap® I; GL Sciences Incorporated, Tokyo, Japan) of 50 μm i.d. and an effective length of 40 cm (50 cm in total) were used with 100 mM Tris–acetate buffer (pH 7.0) containing 0.5% hydroxypropylcellulose as electrophoresis buffers. A P/ACE MDQ CE instrument (Beckman Coulter Incorporated, Brea, CA) was equipped with an argon laser-induced fluorescence detection system with a photometric detection system for fluorescein. The capillary was thermostated at 25 °C. All lectins were dissolved in the running buffer at 1 mg/mL. The capillary was first flushed with a surfactant solution, N102, for 2 min to prevent adsorption of lectin and APTS-labeled oligosaccharides, and then washed with water for 1 min. A solution (~10^{-9} M) of APTS-labeled oligosaccharides was delivered to the capillary for 26 s at 34.5 kPa and the outlet of the capillary was then immersed in a lectin solution and a pressure of 3.45 kPa applied to the outlet of the capillary for 30 s. Fig. 2(A) and the reference electropherograms (Figs. 4 and 5) were obtained without injection of the lectin solution. Neuraminidase digestion was performed in the capillary by injecting neuraminidase solution (3.4 mU/mL) instead of the lectin solution. Both of the reservoirs were changed to the electrophoresis buffer and −15 kV was applied at 25 °C for 30 min. Between the runs, the capillary was rinsed with 0.1 M NaOH at 100 kPa for 10 min, water at 100 kPa for 5 min and the running buffer at 100 kPa for 7 min, in this order. The plug length of the solution in the capillary was calculated using the program CEexpert® supplied by Beckman-Coulter Inc.

2.3. Typical hydrodynamic injection CE as a reference for LVSEP analysis

The capillary was first flushed with the electrophoresis buffer (100 mmol/L Tris–acetate buffer (pH 7.0) containing 0.5% hydroxypropylcellulose). A solution of lectin (1 mg/mL) or neuraminidase (67 mU/mL) was injected at 3.45 kPa for 30 s unless otherwise stated, and an APTS-oligosaccharides solution was injected for 10 s at 3.45 kPa. Sample separation was conducted at −15 kV. The other analytical conditions were the same as those for the LVSEP-PFACE method described above.

3. Results and discussion

3.1. Principle of the LVSEP-PFACE method

The overall LVSEP-PFACE scheme is shown in Fig. 1. In this method, a diluted sample solution of APTS-labeled oligosaccharides is introduced into the entire PDMS-coated capillary (Fig. 1a), then the outlet of the capillary is immersed in a lectin solution and a pressure of 3.45 kPa is applied to introduce a lectin solution for 30 s, which occupies about 22 mm of the 50 cm-long capillary (Fig. 1b). Then, both ends of the capillary are immersed in electrophoresis buffer and the separation voltage is applied (Fig. 1c). Although electroendosmosis in the PDMS-coated capillary is negligible because of the minimal tendency to possess electrical charge, the low concentration of electrolytes in the sample solution induces an electrical charge on the capillary and causes apparent endoosmotic flow (EOF) from anode to cathode (*i.e.*, from outlet to inlet of the capillary) with an EOF velocity of 0.65 mm/s [34]. The EOF velocity decreases gradually as the more high ionic strength electrophoresis buffer solution enters from the outlet of the capillary (Fig. 1d). Concomitantly, the APTS-labeled saccharides, which carry three negatively charged sulfonate groups, will migrate increasingly faster toward the anode and are concentrated in the lectin plug due to the difference in electric field strength between the analyte and the electrophoresis buffer solution. As the electrophoresis buffer approaches the inlet of the capillary and most of the sample matrix is removed from the cathodic end, the EOF becomes negligible, consequently enabling the APTS-labeled oligosaccharides to reach the detector (Fig. 1e). In this step, any oligosaccharides

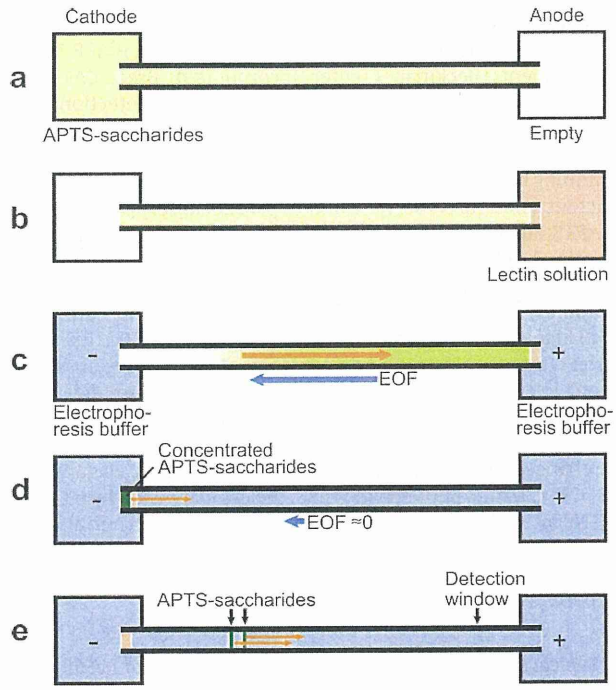

Fig. 1. Image of large-volume sample stacking with partial-filling affinity capillary electrophoresis of APTS-labeled oligosaccharides with lectins, using a neutrally coated capillary. A PDMS-coated capillary was filled with a low ionic strength solution containing APTS saccharides (a). A lectin solution was then injected from the outlet of the capillary as a short plug (b). Both ends of the capillary were immersed in high ionic strength electrophoresis buffer and a negative voltage applied (c). APTS saccharides are enriched at the lectin plug, while the high EOF removes sample matrix from the cathodic end (d). After most of the sample matrix is removed from the cathode end, the EOF becomes negligible and APTS saccharides are separated by zone electrophoresis (e).

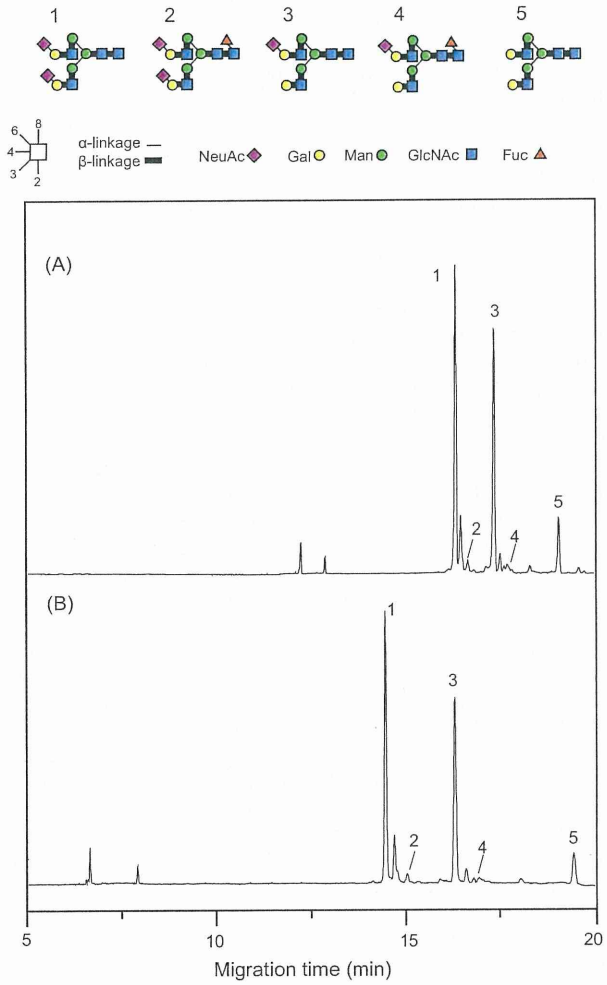

Fig. 2. Electropherograms of the APTS-labeled oligosaccharides derived from human transferrin obtained by LVSEP (A) and ordinary (B) CE. APTS oligosaccharides (0.1 mg/mL as glycoprotein) were injected at 3.45 kPa for 10 s for ordinary CE. LVSEP was performed using 890-fold diluted solution. Conditions: running buffer, 100 mM Tris–acetate buffer, pH 7.0 containing 0.5% hydroxypropylcellulose; capillary, PDMS-coated, 50 μm i.d., 40 cm/50 cm; applied voltage, −15 kV; detection, 488 nm (excitation)/520 nm (emission). Tentative peak assignments were made based on previous work [25].

recognized by lectin are specifically trapped, in contrast to others, which migrate based on their electrophoretic mobilities. Therefore, the oligosaccharides are separated depending on their size and charge ratios, as well as their specific affinities for lectins. The pH at the boundary between the APTS-saccharides solution and lectin phase became basic when voltage was applied, and this denatured the lectins. However, most lectins have isoelectric points in the acidic range, and they slowly moved to the anode without loss of their activity. As expected from the capillary length and the volume of hydrodynamic injection, the concentration factor reaches about a few hundred. The lower limit of detection of the LVSEP method was determined by APTS-labeled maltoheptaose, in which a 3×10^{-10} M solution indicated a signal corresponding to a S/N ratio of 3. This concentration corresponds to one nine hundredths of a hydrodynamic injection at 3.45 kPa for 10 s.

3.2. *Efficiency and repeatability*

The PFACE conditions for APTS-labeled oligosaccharides were optimized as reported previously [25], and it was determined that the PDMS-coated capillary and hydroxypropylcellulose in electrophoresis buffer yielded a good separation by suppressing EOF and preventing adsorption of lectin and APTS-labeled saccharides onto the surface of the PDMS-coated capillary. Adsorption of APTS-saccharides in the preconcentration step could be suppressed by addition of hydroxypropylcellulose to the sample solution. However, for handling convenience, we chose to coat the capillary with N102 surfactant, which also suppressed APTS-saccharide adsorption. During the LVSEP-PFACE method, a lectin and APTS saccharides traveled across the whole capillary in opposite directions. However, no deviation in migration times due to the adsorption of lectins and APTS saccharides on the surface of the capillary was observed, and therefore done all of the work with a single capillary. The generation of EOF was significantly suppressed but electroendosmosis was present with significant velocities, 2.4×10^{-4} and 6.3×10^{-5} $cm^2\,V^{-1}\,s^{-1}$, from anode to cathode in low ionic strength solution and background electrolyte solution (100 mM Tris/acetate, pH 7.0 containing 0.5% hydroxypropylcellulose), respectively. Electrophoretic mobility of APTS saccharides ranges between 2.4×10^{-4} and 8.9×10^{-4} $cm^2\,V^{-1}\,s^{-1}$ in low ionic strength solution (*e.g.* aqueous solution of APTS saccharides). Therefore, all of the APTS saccharides moved and were concentrated in the lectin phase in the LVSEP-PFACE mode.

When a sample solution was introduced by applying a pressure of 34.5 kPa, the capillary was fully filled in 25–26 s. Therefore 26 s was chosen as the injection time for sample solution. The repeatability of the LVSEP-PFACE method was evaluated using APTS-saccharides derived from immunoglobulins, which were

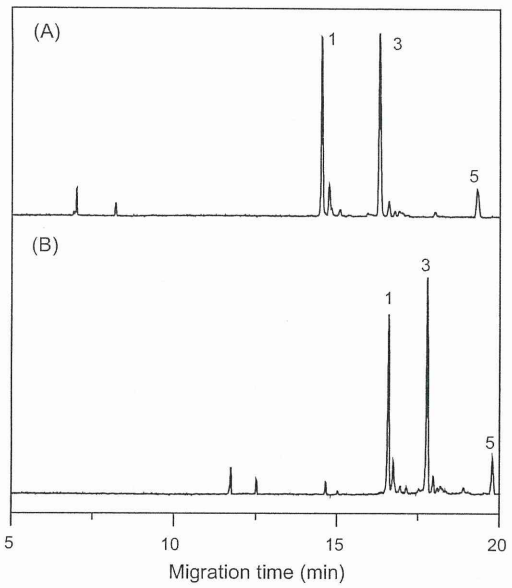

Fig. 3. Electropherograms obtained by ordinary CE (A) and LVSEP CE (B) of APTS-labeled oligosaccharides from transferrin after injection of 67 mU/mL and 3.4 mU/mL of neuraminidase, respectively at 3.45 kPa for 30 s. Other conditions were identical to those used in Fig. 2.

injected into the capillary at 34.5 kPa for 26 s. This was followed by injection of ECA lectin for 30 s at 3.45 kPa from the outlet. The repeatability ($n = 18$), as measured by the RSD, of the migration time ranged from 0.63% to 0.70%, and that of the main peak areas from 5.8% to 6.1% (data not shown). These results indicated that the method had sufficient reliability. Next, the separation efficiency and preconcentration factor were measured by comparing the separation profiles and peak intensities obtained by LVSEP CE and ordinary CE (3.45 kPa for 10 s) without injection of lectins. The data obtained for the transferrin-derived oligosaccharides are shown in Fig. 2. The peak intensities obtained by LVSEP-CE (Fig. 2(A)) were almost the same as those obtained by ordinary CE using a sample solution that was 890 times more concentrated (Fig. 2(B)). Although the separation window for the LVSEP method is narrower than that for ordinary CE, the peak widths for LVSEP were narrower than those obtained by ordinary CE. Therefore, the loss of separation efficiency in LVSEP is negligible. The results indicate this method is reliable.

In the LVSEP-PFACE method, APTS-labeled oligosaccharides are concentrated in the lectin phase and this takes about 2.3 min. By contrast, the residence times of transferrin saccharides in the lectin phase are expected to range from 0.12 min to 0.16 min in ordinary PFACE with injection of a lectin solution for 30 s at 3.45 kPa and then an oligosaccharides solution for 10 s at 3.45 kPa. The increase in the residence time in the lectin phase enhances the efficiency of the interaction. However, the combination of oligosaccharides and lectin does not allow straightforward evaluation of the efficiency of interaction. Here, we chose neuraminidase instead of lectin as a model to compare the efficiency. Injection of 67 mU/mL of neuraminidase for 5 s at 3.45 kPa in an ordinary CE caused a decrease in the peaks of disialylated oligosaccharides appeared at 16.8 min and increases the intensity of the peak at 17.6 min (Fig. 3(A)). The decreased ratio of peak areas indicates *ca.* 10% of the disialylated oligosaccharide was hydrolyzed by the ordinary PFACE mode. In contrast, LVSEP-PFACE using the same amount of oligosaccharides (890 times dilution of the sample) and 3.4 mU/mL neuraminidase indicated almost identical decrease (12%) of disialylated oligosaccharides. More than twenty fold enhancement of

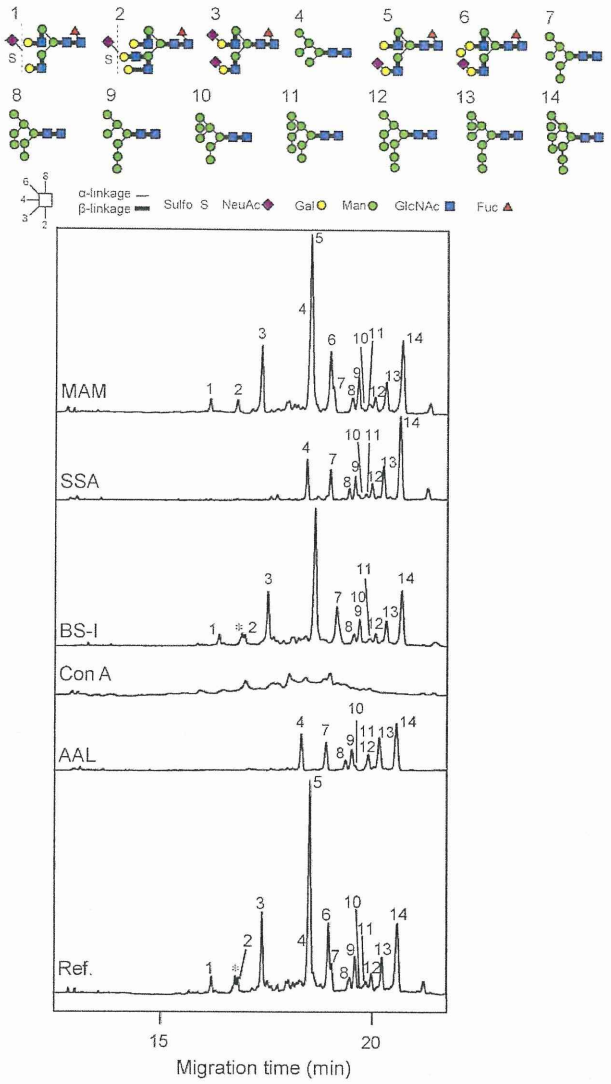

Fig. 4. LVSEP-PFACE analysis of APTS-labeled oligosaccharides derived from porcine thyroglobulin with various lectins under identical conditions. Lectin solution (1 mg/mL) was injected at 3.45 kPa for 30 s. Other analytical conditions were the same as those used in Fig. 2. Tentative peak assignments were made based on previous work [25]. *Indicates unknown structure of oligosaccharide.

enzymatic reaction indicates the efficiency of interaction of the analytes and that partially filled ligand molecules were more potent in the LVSEP process. This result indicates the usefulness of the method.

3.3. LVSEP-PFACE of glycoprotein-derived oligosaccharides

We chose porcine thyroglobulin as oligosaccharide pools and applied these in automated analysis by LVSEP-PFACE using a series of lectin solutions. Thyroglobulin contains a series of high-mannose-type and biantennary complex-type oligosaccharides [35–38]. We chose a series of lectins (MAM, SSA, BS-I, Con A, and AAL) and dissolved these in the running buffer at a concentration of 1 mg/mL (12–110 μM as the concentration of lectins), and introduced them at 3.45 kPa for 30 s, to occupy 22 mm of the 50 cm-long capillary. Having the lectins in excess enables complete interaction of the oligosaccharides with the lectins as reported previously [25]. Migration profiles of the oligosaccharides in the presence of lectins

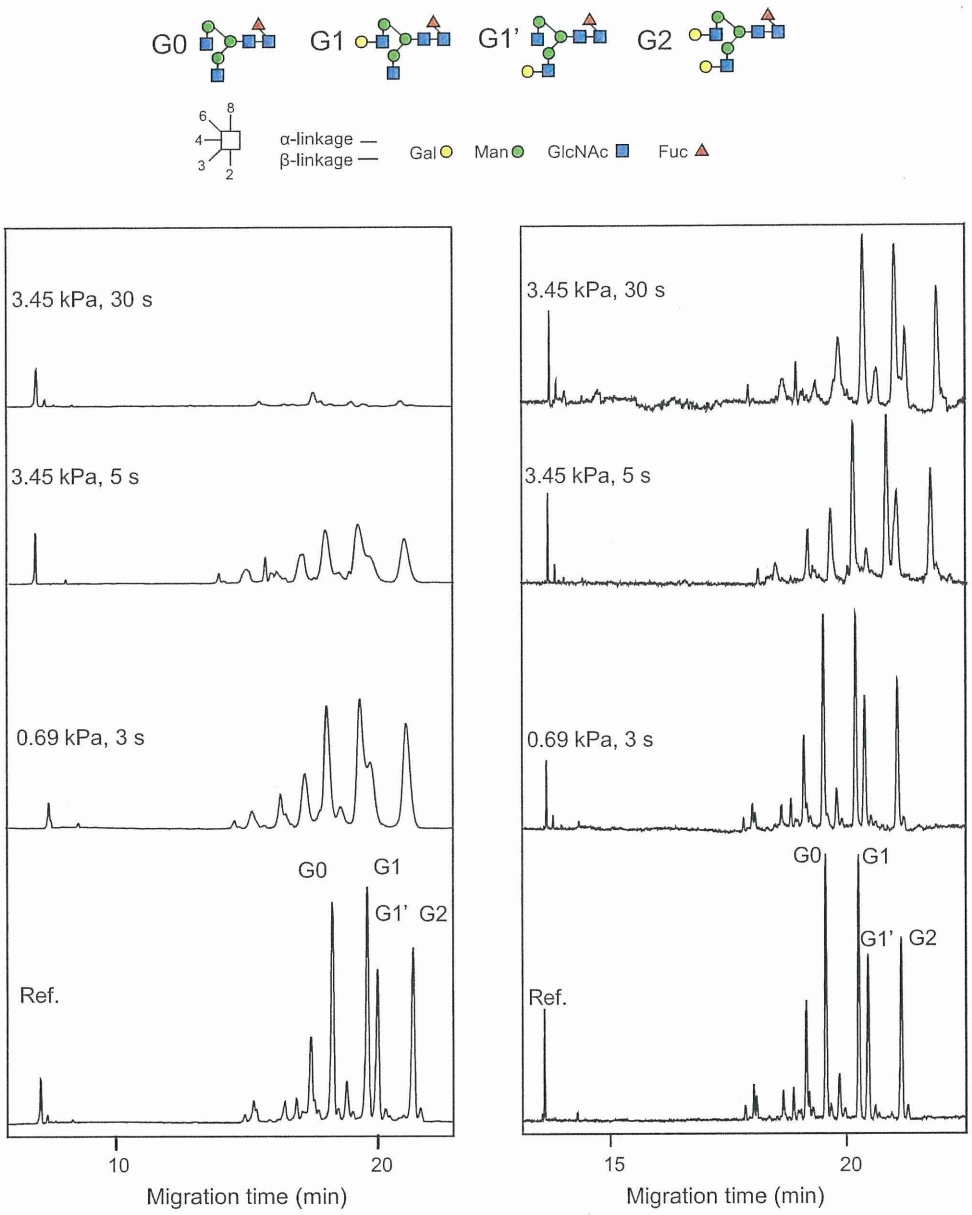

Fig. 5. Comparison of LVSEP-PFACE (left) and ordinary PFACE (right) analysis of APTS-labeled oligosaccharides from immunoglobulin with AAL. Lectin injection conditions are shown in each electropherogram. Other conditions were identical to those used for Fig. 2. Tentative peak assignments were made based on previous work [43].

are shown in Fig. 4. MAM recognizes α2,3-linked NeuAc residues in the non-reducing ends of complex-type oligosaccharides [39]. A peak of oligosaccharide which may contain α2,3-linked NeuAc, marked with an asterisk was completely absent from the electropherogram in thyroglobulin. Addition of α2,6-linked NeuAc specific SSA [40] caused specific disappearance of peaks (peak Nos. 1–3, 5 and 6), which indicated the presence of α2,6-linked NeuAc residues in these saccharides. BS-1 recognizes terminal α-linked Gal. Specific disappearance of a peak (peak No. 6) indicates the presence of terminal α-linked Gal in the oligosaccharides. Con A has strong affinity for high-mannose type oligosaccharides and moderate to weak affinity for biantennary complex type oligosaccharides [41]. Oligosaccharides of thyroglobulin are comprised of high-mannose type and biantennary complex type oligosaccharides. Therefore, all oligosaccharides in thyroglobulin matched the specificity of Con A. As shown in the figure, addition of Con A causes the disappearance of peaks of the series of high-mannose type oligosaccharides and causes severe broadening of other peaks of biantennary complex type oligosaccharides. AAL is a Fuc-binding lectin and the binding strength is high for α1,6-linked Fuc compared with α1,2-linked and α1,3-linked Fuc [42]. Complex-type oligosaccharides (peak Nos. 1–3, 5 and 6) in thyroglobulin contain α1,6-linked Fuc residues in diacetylchitobiose core structure. The electropherogram indicated that peaks 1–3, 5, and 6 in thyroglobulin were recognized by AAL and disappeared from the electropherograms.

The results show that LVSEP-PFACE possesses simple affinity responses. The oligosaccharide peaks recognized by lectins indicate the disappearance or broadening of peaks and does not cause the retardation of the migration time. This is surprising because of the difference from the ordinary PFACE method. In our previous results with ordinary PFACE, Con A and SSA indicated disappearance of specific peaks the same as LVSEP-PFACE. However, study using

other lectins, AAL, ECA, wheat germ agglutinin, *lens culinaris* lectin specific to fucosylated biantennary saccharides, and *Phaseolus vulgaris* agglutinin, indicated an increase in the migration times of specific peaks from 30 s to 2 min. The difference may be due to the effectiveness of the affinity interaction in LVSEP-PFACE compared with the ordinary PFACE method.

The increase in the residence time in the lectin phase in LVSEP-PFACE enhances the efficiency of the interaction. To compare the LVSEP injection and ordinary injection in PFACE analysis, we evaluated the efficiency of affinity CE by changing the injection volumes of lectin in each. In this study, we used immunoglobulin oligosaccharides and AAL as a lectin. Immunoglobulin contains a series of biantennary oligosaccharides with α1,6-linked Fuc in chitobiose core [43,44]. Results are shown in Fig. 5. For the LVSEP-PFACE, the peak intensities of oligosaccharides were reduced with increasing injected amount of lectin (left in Fig. 5). In contrast, ordinary PFACE indicates a gradual broadening and retardation with increasing injection amount of AAL (right in Fig. 5). The difference between the affinity profiles in these two modes may be due to the difference in the interaction profiles. In LVSEP-PFACE, APTS-saccharides are concentrated in the lectin plug for 2.3 min, while the saccharides were continuously supplied from the sample phase and were retained based on the difference in the concentrations of the electrolytes. Therefore, the lectin and saccharides may have interacted under the static conditions. In contrast, during ordinary PFACE, oligosaccharides pass through the lectin phase at *ca.* 0.48 mm/s. Fast mobility of APTS saccharides shortens the contact time with the lectin, which decreases the apparent efficiency of the affinity interaction. Therefore, the advantage of combining the LVSEP mode with PFACE is that the sensitivity is enhanced as well as the interaction efficiency of lectins.

4. Conclusion

The LVSEP-PFACE method can be used effectively to study the interaction between glycoprotein oligosaccharides with some plant lectins with high sensitivity. Use of a PDMS-coated capillary and hydroxypropylcellulose-impregnated electrophoretic buffer enables the generation of an EOF that is significant in low ionic strength solution but negligible in the background electrolyte solution. This phenomenon enables effective preconcentration by LVSEP and good resolution of APTS derivatives of glycoprotein-derived oligosaccharides. The preconcentration efficiency reached a factor of *ca.* 900 compared to typical injection at 3.45 kPa, 10 s, enabling the enhanced detection of oligosaccharides. The residence time of APTS saccharides in the lectin phase is substantially increased during the preconcentration step, which enhances the efficiency of the affinity interaction. The simplicity and high-sensitivity of this method should be of value for monitoring the changes in oligosaccharides in various situations. Therefore, combination of LVSEP method with PFACE and ordinary CE will be useful in profiling of minor components in the glycan pool because it does not require preconcentration of the sample solution. We believe this will be helpful in analysis of glycans in various glycoproteinaceous pharmaceuticals.

Acknowledgments

This work was supported by a Grant-in-Aid for Scientific Research (C) from the Japan Society for the Promotion of Science (JSPS), and the "High-Tech Research Center" Project for Private Universities: a matching fund subsidy from the Ministry of Education, Culture, Sports, Science and Technology (MEXT), Japan, 2007–2011.

References

[1] A. Varki, R. Cummings, J. Esko, H. Freeze, G. Hart, J. Marth, Essentials of Glycobiology, Cold Spring Harber Laboratory Press, New York, 1999.
[2] A. Knezevic, O. Polasek, O. Gornik, I. Rudan, H. Campbell, C. Hayward, A. Wright, I. Kolcic, N. O'Donoghue, J. Bones, P.M. Rudd, G. Lauc, J. Proteome Res. 8 (2009) 694.
[3] A. Larkin, B. Imperiali, Biochemistry 50 (2011) 4411.
[4] M. Molinari, Nat. Chem. Biol. 3 (2007) 313.
[5] D. Skropeta, Bioorg. Med. Chem. 17 (2009) 2645.
[6] R.J. Sola, K. Griebenow, J. Pharm. Sci. 98 (2009) 1223.
[7] B.M. Kumpel, T.W. Rademacher, G.A. Rook, P.J. Williams, I.B. Wilson, Hum. Antibodies Hybridomas 5 (1994) 143.
[8] B.M. Kumpel, Y. Wang, H.L. Griffiths, A.G. Hardley, G.A. Rook, Hum. Antibodies Hybridomas 6 (1995) 82.
[9] P. Umana, J. Jean-Mairet, R. Moudry, H. Amstutz, J.E. Bailey, Nat. Biotechnol. 17 (1999) 176.
[10] J. Davies, L. Jiang, L.Z. Pan, M.J. LaBarre, D. Anderson, M. Reff, Biotechnol. Bioeng. 74 (2001) 288.
[11] R.L. Shields, J. Lai, R. Keck, L.Y. O'Connell, K. Hong, Y.G. Meng, S.H.A. Weikert, L.G. Presta, J. Biol. Chem. 277 (2002) 26733.
[12] T. Shinkawa, K. Nakamura, N. Yamane, E. Shoji-Hosaka, Y. Kanda, M. Sakurada, K. Uchida, H. Anazawa, M. Satoh, M. Yamasaki, N. Hanai, K. Shitara, J. Biol. Chem. 278 (2003) 3466.
[13] M.E. Janik, A. Litynska, P. Vereecken, Biochim. Biophys. Acta 1800 (2010) 545.
[14] F. Tousi, W.S. Hancock, M. Hincapie, Anal. Methods 3 (2011) 20.
[15] R.P. Estrella, J.M. Whitelock, R.H. Roubin, N.H. Packer, N.G. Karlsson, Methods Mol. Biol. 534 (2009) 171.
[16] E. Gelpi, J. Chromatogr. A 703 (1995) 59.
[17] H. Karlsson, J.M. Larsson, K.A. Thomsson, I. Hard, M. Backstrom, G.C. Hansson, Methods Mol. Biol. 534 (2009) 117.
[18] A. Kondo, W. Li, T. Nakagawa, M. Nakano, N. Koyama, X. Wang, J. Gu, E. Miyoshi, N. Taniguchi, Biochim. Biophys. Acta 1764 (2006) 1881.
[19] M. Wuhrer, A.M. Deelder, C.H. Hokke, J. Chromatogr. B 825 (2005) 124.
[20] H. Lis, N. Sharon, Annu. Rev. Biochem. 42 (1973) 541.
[21] Z. Dai, J. Zhou, S.J. Qiu, Y.K. Liu, J. Fan, Electrophoresis 30 (2009) 2957.
[22] M. Militsopoulou, F. Lamari, N.K. Karamanos, J. Pharm. Biomed. Anal. 32 (2003) 823.
[23] K. Nakajima, M. Kinoshita, N. Matsushita, T. Urashima, M. Suzuki, A. Suzuki, K. Kakehi, Anal. Biochem. 348 (2006) 105.
[24] K. Nakajima, M. Kinoshita, Y. Oda, T. Masuko, H. Kaku, N. Shibuya, K. Kakehi, Glycobiology 14 (2004) 793.
[25] S. Yamamoto, C. Shinohara, E. Fukushima, K. Kakehi, T. Hayakawa, S. Suzuki, J. Chromatogr. A 1218 (2011) 4772.
[26] T. Kawai, K. Sueyoshi, F. Kitagawa, K. Otsuka, Anal. Chem. 82 (2010) 6504.
[27] K. Choi, Y.G. Jin, D.S. Chung, J. Chromatogr. A 1216 (2009) 6466.
[28] Z. Zhu, L. Zhang, A. Marimuthu, Z. Yang, Electrophoresis 23 (2002) 2880.
[29] G. Danger, R. Pascal, H. Cottet, J. Chromatogr. A 1216 (2009) 5748.
[30] B. Kim, D.S. Chung, Electrophoresis 23 (2002) 49.
[31] Z. Wang, C. Liu, J. Kang, J. Chromatogr. A 1218 (2011) 1775.
[32] Y. He, H.K. Lee, Anal. Chem. 71 (1999) 995.
[33] G. McGrath, W.F. Smyth, J. Chromatogr. B 681 (1996) 125.
[34] A.R. Wheeler, G. Trapp, O. Trapp, R.N. Zare, Electrophoresis 25 (2004) 1120.
[35] P. deWaard, A. Koorevaar, J.P. Kamerling, J.F.G. Vliegenthart, J. Biol. Chem. 266 (1991) 4237.
[36] K. Yamamoto, T. Tsuji, T. Irimura, T. Osawa, Biochem. J. 195 (1981) 701.
[37] T. Tsuji, K. Yamamoto, T. Irimura, T. Osawa, Biochem. J. 195 (1981) 691.
[38] J. Charlwood, H. Birrell, A. Organ, P. Camilleri, Rapid Commun. Mass Spectrom. (1999) 716.
[39] R.N. Knibbs, I.J. Goldstein, R.M. Ratcliffe, N. Shibuya, J. Biol. Chem. 266 (1991) 83.
[40] K. Tazaki, N. Shibuya, Plant Cell Physiol. 30 (1989) 899.
[41] C.F. Brewer, L. Bhattacharyya, J. Biol. Chem. 261 (1986) 7306.
[42] K. Yasmashita, N. Kochibe, T. Ohkura, I. Ueda, A. Kobata, J. Biol. Chem. 260 (1985) 4688.
[43] Y. Yagi, S. Yamamoto, K. Kakehi, T. Hayakawa, Y. Ohyama, S. Suzuki, Electrophoresis 32 (2011) 2979.
[44] L.A. Gennaro, O. Salas-Solano, S. Ma, Anal. Biochem. 355 (2006) 249.

Analytical Biochemistry 431 (2012) 120–126

Contents lists available at SciVerse ScienceDirect

Analytical Biochemistry

journal homepage: www.elsevier.com/locate/yabio

Specific detection of *N*-glycolylneuraminic acid and Galα1–3Gal epitopes of therapeutic antibodies by partial-filling capillary electrophoresis

Yuki Yagi [a,*], Kazuaki Kakehi [b], Takao Hayakawa [b], Yukihito Ohyama [a], Shigeo Suzuki [b]

[a] *Kyowa Hakko Kirin Co., Ltd., Takasaki, Gunma 370-0013, Japan*
[b] *Faculty of Pharmaceutical Sciences, Kinki University, Higashi-Osaka, Japan*

ARTICLE INFO

Article history:
Received 4 June 2012
Received in revised form 1 September 2012
Accepted 4 September 2012
Available online 11 September 2012

Keywords:
N-glycolylneuraminic acid
Galα1–3Gal
Myeloma cells
Immunoglobulin
Oligosaccharide
Partial-filling affinity electrophoresis

ABSTRACT

The oligosaccharide structure is very important in biopharmaceuticals because of its effects on protein function, including efficacy and half-life. *N*-Glycolylneuraminic acid (Neu5Gc) and Galα1–3Gal (α-Gal) residues are known to show immunogenicity in humans. It is now understood that murine cell lines, such as NS0 or SP2, which are typically used for biopharmaceutical manufacture, produce proteins containing Neu5Gc and α-Gal residues. The expression of these specific residues is affected by the cell line and culture conditions. Therefore, monitoring and controlling the levels of these epitopes are important for the quality control of biopharmaceuticals. To detect the two epitopes on a therapeutic antibody produced by NS0 cells, we applied partial-filling capillary electrophoresis using anti-Neu5Gc antibody and α-galactosidase. In the anti-Neu5Gc antibody filling method, one minor glycan peak with Neu5Gc residues at the nonreducing end disappeared specifically from the electropherogram. In the α-galactosidase filling method, some minor peaks with α1,3-linked Gal residues disappeared. However, in a therapeutic antibody from Chinese hamster ovary cells, no peaks disappeared with the two methods. These results show this method can be used to specifically detect and quantify the two epitopes on biopharmaceuticals with high sensitivity.

More than 20 pharmaceutical antibodies have been approved for treatment of cancers, autoimmune disorders, and inflammation [1,2]. Antibodies are becoming important agents for medical treatment because of their high specificity and low toxicity. Antibody molecules contain glycosylation sites that bear various oligosaccharides depending on the cell lines used for antibody production [3,4].

Some therapeutic antibodies produced by mouse myeloma cells, such as SP2 or NS0 cells, are known to generate *N*-glycolylneuraminic acid (Neu5Gc)[1] and Galα1–3Gal (α-Gal), which show immunogenicity in humans [5–11]. In addition, some reported Chinese hamster ovary (CHO) cells can produce α-Gal [12,13]. Neu5Gc is known to induce immune responses in humans. Anti-Neu5Gc antibodies have been detected in 85% of the human population, sometimes at high levels [14,15,10]. In addition, high Neu5Gc levels on proteins are associated with rapid clearance profiles in vivo [16]. α-Gal is strongly immunogenic in humans and over 1% of serum IgG is directed against the residue [17]. The presence of α-Gal attributed to a murine myeloma cell line mainly causes adverse clinical events associated with an induced IgE-mediated anaphylaxis response in patients treated with the commercial antibody cetuximab [18,19]. Some reports suggest that these glycan epitope expressions are affected by cell lines and culture conditions [6,7,20–22]. Controlling the levels of this antigenic epitope during development of biotherapeutics could have a positive impact on the safety and clearance of the drug.

Several analytical techniques have been used for detection and quantification of the glycan epitopes. These include high-pH anion-exchange chromatography with pulsed amperometric detection [23], HPLC with fluorescence labeling [24], liquid chromatography coupled with MS [13,25–27], enzyme-linked immunosorbent assay [28,29], and detection by lectins [30–33]. However, there are few cases in which capillary electrophoresis has been used for detection of the epitopes. Capillary electrophoresis with laser-induced fluorescence detection (CE-LIF) provides rapid, high-resolution, and highly sensitive analysis of fluorescence-labeled oligosaccharides. In particular, 8-aminopyrene-1,3,6-trisulfonate (APTS) has been widely used for analysis of oligosaccharides derived from antibody pharmaceuticals [34–39]. Three sulfonate groups of APTS induce rapid movement of labeled oligosaccharides, and the oligosaccharides in antibodies undergo complete resolution by CE-LIF. In addition, the partial-filling technique has been used to ascertain the affinity characteristics between receptors and ligands [40–53]. In this technique, the capillary is partly filled with the affinity ligand dissolved in running buffer before injection of the sample. The pH of the running buffer is selected to sustain the affinity of ligand proteins, and the sample must be moved quickly across the "plug" of ligand in an electric

* Corresponding author. Fax: +81 27 352 4977.
E-mail address: yuuki.yagi@kyowa-kirin.co.jp (Y. Yagi).

[1] *Abbreviations used:* Neu5Gc, *N*-glycolylneuraminic acid; α-Gal, Galα1–3Gal; CHO, Chinese hamster ovary; CE-LIF, capillary electrophoresis with laser-induced fluorescence detection; APTS, 8-aminopyrene-1,3,6-trisulfonic acid; GSL I-B_4, *Griffonia simplicifolia* I-B_4; PFACE, partial-filling affinity capillary electrophoresis.

0003-2697/$ - see front matter © 2012 Elsevier Inc. All rights reserved.
http://dx.doi.org/10.1016/j.ab.2012.09.006

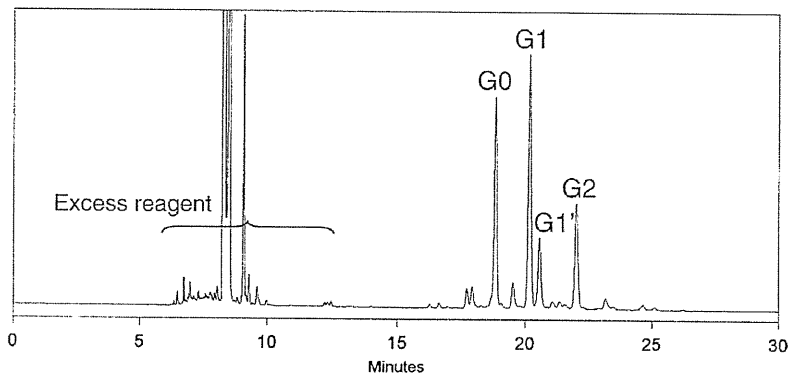

Fig.1. Typical electropherogram of APTS-labeled oligosaccharides derived from palivizumab. Analytical conditions: capillary, DB-1 (total length, 40 cm; effective length, 30 cm; 50 μm i.d.); running buffer, 100 mM Tris–acetic acid buffer (pH 7.0) with 0.05% hydroxypropyl cellulose; applied voltage, −15 kV at 25 °C; sample injection, 3.4 kPa, for 15 s.

field. When a voltage is applied, the sample migrates through the plug of affinity ligand. Sample components with affinity to the ligand phase are trapped, and those that do not have affinity reach the detector without retardation. This technique does not require chemical immobilization of the ligand molecules.

In an earlier study, we applied the partial-filling affinity capillary electrophoresis (PFACE) method with lectins and enzymes for the analysis of APTS-labeled oligosaccharides obtained from a therapeutic antibody [54]. However, there are no lectins and enzymes that specifically interact or react with the Neu5Gc residue. Therefore, in this study, we applied the anti-Neu5Gc antibody to the PFACE method. In addition, because of the unknown specificity of *Griffonia simplicifolia* I-B_4 (GSL I-B_4), which is currently used for detection of α-Gal in histochemistry [30–33], we chose α-galactosidase for detection of α-Gal residues.

Materials and methods

Materials

The following materials were used in this study: palivizumab (Medimmune, Gaithersburg, MD, USA), rituximab (Genentech, San Francisco, CA, USA), *N*-glycosidase F (Roche Diagnostics, Mannheim, Germany), APTS (Beckman–Coulter, Fullerton, CA, USA), acetic acid and tetrahydrofuran (Wako Pure Chemical Industries, Tokyo, Japan), sodium cyanoborohydride (Sigma–Aldrich, St. Louis, MO, USA), hydroxypropyl cellulose (3–6 mPa/s; Tokyo Chemical Industry Co., Ltd, Tokyo, Japan), DB-1 capillary (J&W Scientific, Folsom, CA, USA), NAP-5 columns (GE Healthcare Life Sciences, Piscataway, NJ, USA), 2-mercaptoethanol (Nacalai Tesque, Tokyo, Japan), anti-Neu5Gc polyclonal antibody (Sialix, Vista, CA, USA), α2-3,6,8,9-neuraminidase (*Arthrobacter ureafaciens*) (Nacalai Tesque), lectin from GSL I-B_4 (Vector Laboratories, Burlingame, CA, USA), α1–3,4,6-galactosidase (green coffee bean) (ProZyme, Hayward, CA, USA), and β1–4-galactosidase (Calbiochem, Hayward, CA, USA).

Release of N-linked oligosaccharides from therapeutic antibodies

Antibody (50 μl, 500 μg) was mixed with 2-mercaptethanol (1 μl) and 1 U/μl of *N*-glycosidase F (15 μl). The mixture was incubated at 37 °C overnight. After digestion, 154 μl of ice-cold ethanol was added, and the mixture was centrifuged (10,000*g* for 15 min at 4 °C) to remove proteins. The supernatant was dried using a centrifugal vacuum evaporator.

Fluorescence derivatization of oligosaccharides with APTS

Oligosaccharides were labeled according to an established method [54]. Briefly, the dry sample was dissolved in 3 μl of 0.2 M APTS in 15% (v/v) acetic acid and then mixed with 3 μl

Table 1
Structures of the major oligosaccharides derived from palivizumab and their relative corrected peak areas.

Name	Structure	Relative corrected peak area (%)
G0	GlcNAcβ1-2Manα1\6 Fucα1\6 GlcNAcβ1-2Manα1/3 Manβ1-4GlcNAcβ1-4GlcNAc	26.9
G1	Galβ1-4GlcNAcβ1-2Manα1\6 Fucα1\6 GlcNAcβ1-2Manα1/3 Manβ1-4GlcNAcβ1-4GlcNAc	32.4
G1'	GlcNAcβ1-2Manα1\6 Fucα1\6 Galβ1-4GlcNAcβ1-2Manα1/3 Manβ1-4GlcNAcβ1-4GlcNAc	10.0
G2	Galβ1-4GlcNAcβ1-2Manα1\6 Fucα1\6 Galβ1-4GlcNAcβ1-2Manα1/3 Manβ1-4GlcNAcβ1-4GlcNAc	13.2

The relative corrected peak area (%) was calculated as follows: corrected peak area = (measured peak area)/(migration time), relative corrected peak area (%) = [(corrected peak area)/(total corrected peak area)] × 100.

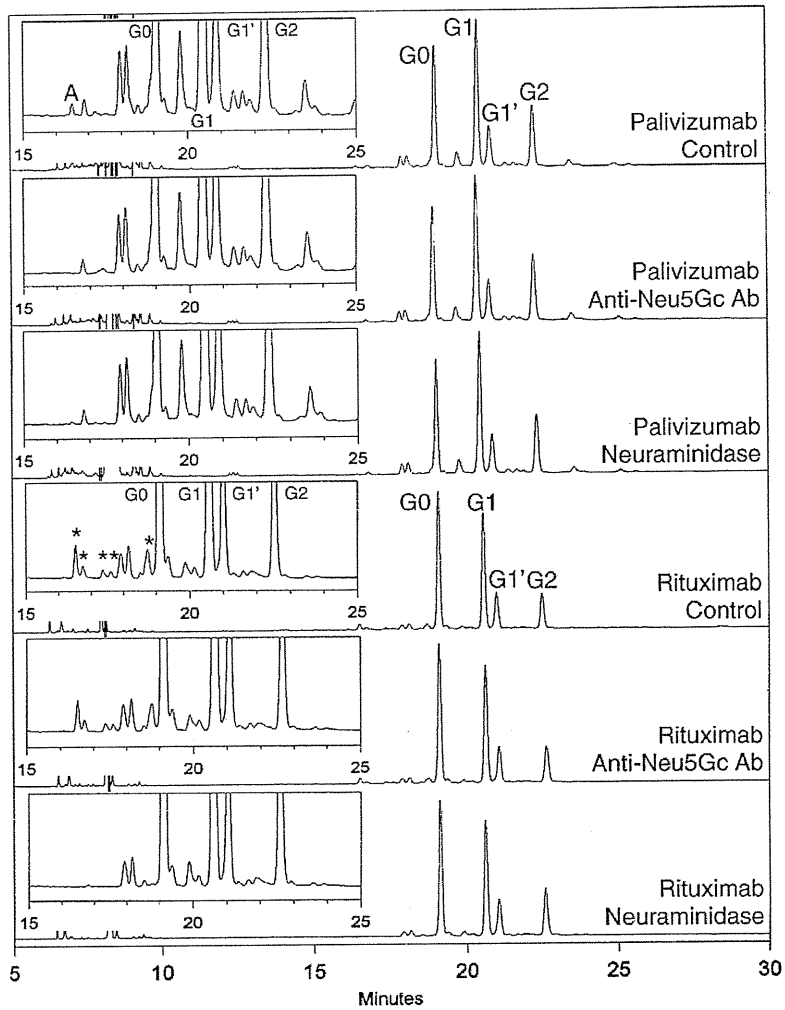

Fig.2. Partial-filling affinity electrophoresis with anti-Neu5Gc antibody (Ab) and partial-filling enzymatic digestion with α2–3,6,8,9-neuraminidase (5 U/ml) of APTS-labeled oligosaccharides from palivizumab and rituximab. Capillary electrophoresis conditions: lectin injection, 3.4 kPa, for 60 s. Other conditions were identical to those for Fig. 1.

of a 1 M sodium cyanoborohydride solution in tetrahydrofuran. The mixture was heated at 55 °C for 90 min and then mixed with 94 μl of water before being applied to a NAP-5 column previously equilibrated with 10 ml of water. APTS–oligosaccharides were recovered by elution with 600 μl of water. The eluate from the column was dried with a centrifugal vacuum evaporator, and the residue was dissolved in 1 ml of water for capillary electrophoresis.

Capillary electrophoresis of APTS-labeled oligosaccharides

The capillary electrophoresis system used in this study was a PA-800 system (Beckman–Coulter) with an argon laser-induced fluorescence detector (excitation wavelength 488 nm; emission wavelength 520 nm). A DB-1 capillary (50 μm i.d.; effective length, 30 cm; total length, 40 cm) was used with 100 mM Tris–acetic acid buffer (pH 7.0) with 0.05% hydroxypropyl cellulose as the running buffer. Sample solutions were introduced to the capillary under pressure (3.4 kPa). A voltage of −15 kV was applied at 25 °C for 30 min. Before each run, the capillary was rinsed with 0.1 M NaOH at 103 kPa for 10 min, water at 103 kPa for 5 min, and the running buffer at 103 kPa for 7 min.

Partial-filling capillary electrophoresis

Antibody, lectin, and enzymes were diluted with the running buffer. Before a sample solution was introduced, the antibody (or lectin, enzyme) solution was introduced into the capillary under pressure (3.4 kPa; 60 s). The samples were separated under the same conditions as described above.

Results and discussion

CE-LIF analysis of N-linked glycan structure from palivizumab

Palivizumab, which is a recombinant antibody against respiratory syncytial virus, has an N-linked oligosaccharide at each Fc region. A typical electropherogram for the analysis of APTS-labeled oligosaccharides from palivizumab is shown in Fig. 1. Peaks appeared between 6 and 13 min for the reagents, while peaks for the APTS-labeled oligosaccharides were observed between 16 and 26 min. The main oligosaccharides of palivizumab and their corrected peak areas are shown in Table 1. Palivizumab contains the following four major oligosaccharides: G0, an agalactosylated oligosaccharide; G1 and G1′, monogalactosylated oligosaccharides

II NeuAcα2-6{Galβ1-4GlcNAcβ1-2Manα1\6, Galβ1-4GlcNAcβ1-2Manα1/3} Manβ1-4GlcNAcβ1-4GlcNAc, Fucα1\6

III Galα1-3 NeuAcα2-6{Galβ1-4GlcNAcβ1-2Manα1\6, Galβ1-4GlcNAcβ1-2Manα1/3} Manβ1-4GlcNAcβ1-4GlcNAc, Fucα1\6

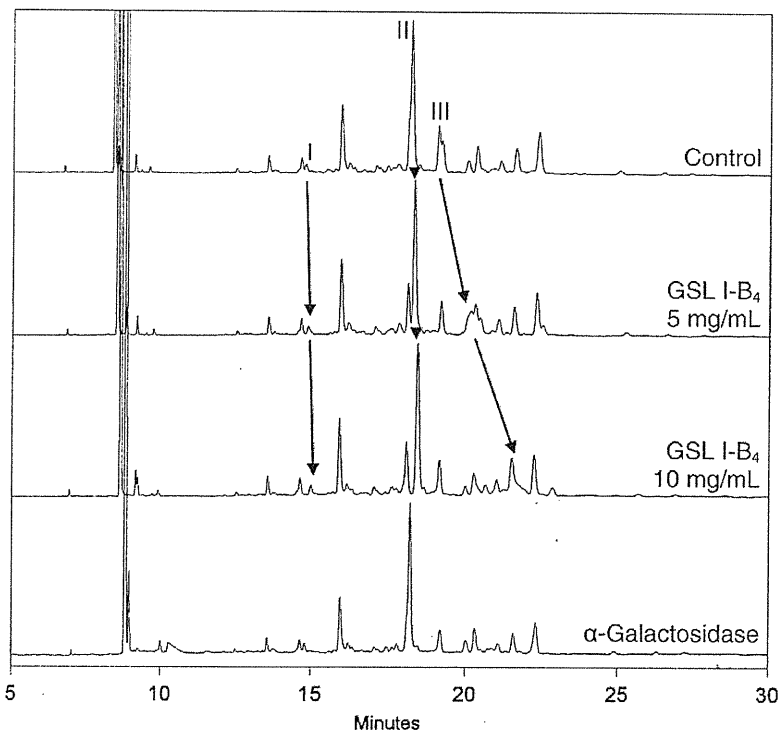

Fig.3. Partial-filling affinity electrophoresis with GSL I-B_4 and partial-filling enzymatic digestion with α1–3,4,6-galactosidase (75 U/ml) of APTS-labeled oligosaccharides from porcine thyroglobulin. Capillary electrophoresis conditions were identical to those for Fig. 2.

with two positional isomers; and G2, a fully galactosylated oligosaccharide. In addition, palivizumab should have some Neu5Gc and α-Gal at the nonreducing terminals of its N-linked glycan because the antibody is produced from NS0 cells [5–8].

We have previously shown that CE-LIF is suitable for the determination and characterization of APTS oligosaccharides derived from an antibody, because it has high reproducibility [54]. The results showed high reproducibility, with relative SDs of less than 0.6% (SD $\leqslant$ 0.1%) for the relative corrected peak areas and less than 0.1% for migration times with three independent preparations from rituximab, which is a recombinant antibody used for the treatment of non-Hodgkin lymphoma.

Specific detection of Neu5Gc residues using PFACE with anti-Neu5Gc antibody

Because there are no lectins or enzymes that interact with or hydrolyze Neu5Gc residues specifically, we used anti-Neu5Gc antibody, which is a chicken polyclonal IgY [55]. This antibody is highly specific to Neu5Gc residues found in oligosaccharides and glycoproteins. After introduction of 2.6 μM anti-Neu5Gc antibody solution to the capillary, the APTS-labeled oligosaccharides from palivizumab were injected and separated. The resultant electropherogram (Fig. 2) showed that anti-Neu5Gc antibody caused the disappearance of a minor peak at around 16.5 min (peak A). The corrected peak area ratio of peak A to total saccharide peaks was 0.4%. Peak A disappeared after partial-filling enzymatic digestion [54] with α2–3,6,8,9-neuraminidase. These results show that peak A is a glycan with Neu5Gc residues at the nonreducing ends. By contrast, though some glycan peaks, marked by asterisks, from rituximab produced from CHO cells disappeared after digestion with α2–3,6,8,9-neuraminidase, no peaks disappeared with preinjection of anti-Neu5Gc antibody (Fig. 2). This result shows that rituximab has no Neu5Gc residues and is consistent with an earlier detailed study of the glycan profile of rituximab [56].

These studies confirmed that PFACE with anti-Neu5Gc antibody can detect Neu5Gc residues on oligosaccharides from biopharmaceuticals with high specificity and sensitivity. In addition, the combination of PFACE with various kinds of lectins and exoglycosidases will provide additional detailed information about glycan branches [54].

Specific detection of α-Gal residues using partial-filling enzymatic digestion in capillary electrophoresis with α-galactosidase

GSL I-B_4 is specific for terminal α-Gal residues and is used to detect the α-Gal epitope in xenotransplantation research [30,33]. However, when evaluating the specificity of this lectin to porcine thyroglobulin, we surprisingly observed unfamiliar specificity of this lectin. Partial-filling GSL I-B_4 capillary electrophoresis of saccharides from porcine thyroglobulin showed weak interaction with a monosialylated biantennary complex-type glycan (peak II) which